arXiv:astro-ph/9909414v1 24 Sep 1999

Probing Neutrino Properties with the Cosmic Microwave Background

Robert E. Lopez*
Department of Physics
University of Chicago
Chicago, IL 60637

(Dated: February 1, 2008)

Neutrinos that decay leave their imprint on the cosmic microwave background. We calculate the CMB anisotropy for the full range of decaying neutrino parameter space, and investigate the ability of future experiments like MAP and Planck to probe decaying neutrino physics. We adopt two approaches: distinguishing decaying neutrino models from fiducial ΛCDM, and measuring neutrino parameters. With temperature data alone, MAP can distinguish stable neutrino models from ΛCDM if the neutrino mass $m_h \gtrsim 2$ eV. Adding polarization data, $m_h \gtrsim 0.5$ eV is distinguishable. Planck can distinguish $m_h \gtrsim 0.5$ eV with temperature alone, and $m_h > 0.25$ eV with polarization. MAP without polarization can distinguish out-of-equilibrium, early-decaying models as long as $(m_h/\mathrm{MeV})^2\,\mathrm{t_d}/\mathrm{sec} \gtrsim 230$, and with polarization if $(m_h/\mathrm{MeV})^2\,\mathrm{t_d}/\mathrm{sec} \gtrsim 150$. For Planck without polarization, models with $(m_h/\mathrm{MeV})^2\,\mathrm{t_d}/\mathrm{sec} \gtrsim 9$ are distinguishable, and with polarization if $(m_h/\mathrm{MeV})^2\,\mathrm{t_d}/\mathrm{sec} \gtrsim 6$. Models in which neutrinos decay in equilibrium are indistinguishable from ΛCDM. Late-decaying models ($10^{13}\mathrm{sec} \lesssim \mathrm{t_d} \lesssim 4\times10^{17}\mathrm{sec}$) are distinguishable from ΛCDM if $m_h \gtrsim 5$ eV for MAP and $m_h \gtrsim 2$ eV for Planck. Adding decaying neutrino parameters to the set of cosmic parameters, we calculate the statistical uncertainty in the full set of cosmic parameters. The ability to measure neutrino parameters depends sensitively on the decaying neutrino model. Adding neutrino parameters degrades the sensitivity to non-neutrino parameters; the relative amount of sensitivity degradation depends on the decaying neutrino model, but tends to decrease with increasing experimental sensitivity.

I. INTRODUCTION

The anisotropy in the cosmic microwave background (CMB) can be a powerful probe of the early universe. Currently available data has already been used to place interesting constraints on cosmic parameters [1, 2, 3, 4, 5, 6, 7, 8, 9, 10, 11, 12], and with the advent of exquisitely sensitive satellite-based experiments like MAP [13] and Planck [14], it is possible to envision using the CMB to go beyond standard parameter estimation. Many such examples have been considered: detecting finite-temperature QED effects [15], constraining variations in the fine-structure constant [16], placing limits on lepton asymmetry [17], and constraining Brans-Dicke theories [18]. Another possibility is to use the CMB to probe decaying neutrinos.

Decaying neutrinos have been considered in several cosmological contexts such as big-bang nucleosynthesis [19, 20, 21, 22, 23], large-scale structure formation [24, 25, 26, 27, 28] and the CMB. The CMB anisotropy for models in which the neutrino decays before recombination, $t_d \ll t_{rec} \simeq 10^{13}$ sec, have been calculated [27, 29, 30, 31]. Current CMB data have been used to study to late-decaying models, where $t_d \gtrsim 10^{13}$ sec, with the result that masses $m_h > 100$ eV are mostly excluded [32, 33]. Late-decaying neutrinos have also been studied in the context of future CMB experiments [31]. However, as pointed out in reference [32], previous calculations all treated the decay radiation perturbations as equivalent to those of the massless neutrinos. This approximation is only valid for early-decaying scenarios. A systematic study of the CMB anisotropy in decaying neutrino models is needed.

This work explores the use of future CMB observations, like the MAP and Planck experiments, to probe decaying neutrino physics over a large range of neutrino parameter space. It is organized as follows: First, we briefly discuss models of neutrino decay in Sec. II. We describe the extra steps required to calculate the CMB spectra in Sec. III. In Sec. IV, we briefly review cosmic parameter estimation and ruling out models in the linear regime; the formalism used to rule out models is developed in the Appendix. We discuss how the physics of CMB anisotropy varies as a function of neutrino mass and lifetime in Sec V. This is used to break the neutrino parameter space into regions where the physics of the CMB anisotropy is similar. We then present results: distinguishing decaying neutrino models from standard models, and measuring cosmic parameters in Sec. VI.

---

*r-lopez@uchicago.edu; this paper represents partial fulfillment of the requirements for the Ph.D. in Physics at the University of Chicago

II. MASSIVE NEUTRINOS

The evidence for neutrino mass from atmospheric, solar and direct-beam neutrino oscillation experiments is compelling[55], and massive neutrinos tend to decay unless protected by some symmetry. It is therefore interesting to consider the cosmological signature of decaying neutrinos.

In this work we will consider neutrinos that decay non-radiatively into light decay products. By non-radiative we mean that the decay products are electromagnetically non-interacting. Radiative decay channels could also exist, e.g., $\nu_h \rightarrow \nu_l \gamma$ or $\nu_h \rightarrow e^+ e^- \nu_l$. However, these models are generally excluded by observations unless the lifetimes are extremely long [35, 36]; the region of parameter space that can be probed by the CMB is certainly excluded. There are several models with non-radiative decay products that are motivated by particle physics. For example, familon models [37, 38, 39] predict the following decay process: $\nu_h \rightarrow \nu_l \phi$ where ϕ is a familon, a massless Nambu-Goldstone boson associated with spontaneous breaking of a continuous, global family symmetry. In these models, the decaying neutrino mass and mean lifetime are related at tree level by

$$t_d = \frac{16\pi}{m_h} \left(\frac{F}{m_h} \right)^2 , \tag{1}$$

where F is the energy scale at which the family symmetry is broken, and it is assumed that the neutrino ν_l is much lighter. This interaction induces a corresponding charged-lepton decay, and experimental constraints on their branching ratios can be used to set lower bounds on F. Familons corresponding to a μ-τ family symmetry are the least well constrained: the branching ratio $B(\tau \rightarrow \mu\phi) \lesssim 3 \times 10^{-3}$ [40] which implies that $F \gtrsim 4 \times 10^6$ GeV for the second-third family symmetry. This leads to the following constraint, assuming that $\nu_h = \nu_\tau$ and $\nu_l = \nu_\mu$:

$$\left(\frac{t_d}{\mathrm{sec}} \right) \left(\frac{m_h}{\mathrm{eV}} \right)^3 > 3.0 \times 10^{17} . \tag{2}$$

Much of the decaying neutrino parameter space that can be probed by the CMB satisfies this constraint.

In models where neutrinos acquire mass through the see-saw mechanism, the three-body decay $\nu_h \rightarrow \nu_l \nu_l \bar{\nu}_l$ can occur [36], mediated by the exchange of a Z-boson. However, the lifetime for this decay,

$$\frac{t_d}{\mathrm{sec}} \sim 10^{30} \left(\frac{\mathrm{eV}}{m_h} \right)^5 , \tag{3}$$

is so large that the neutrino is effectively stable over the interesting region of parameter space.

Motivated by the discussion above, we consider the following decay channel throughout this work: $\nu_h \rightarrow \nu_l \phi$. However, alternate decay processes, like the aforementioned $\nu_h \rightarrow \nu_l \nu_l \bar{\nu}_l$ do not alter our results much; the small differences are discussed where they exist. Therefore, it is appropriate to specify decaying neutrino models by m_h and t_d alone. The results are then model-independent for most of the interesting parameter space.

III. CALCULATING THE ANISOTROPY

The anisotropy in the effective temperature of the CMB radiation, δT, is typically described in terms of spherical harmonics,

$$\frac{\delta T(\theta, \phi)}{T_0} = \sum_{lm} a^T_{lm} Y_{lm}(\theta, \phi) , \tag{4}$$

where θ and ϕ describe the position on the sky, and $T_0 = 2.728$ K is the mean background temperature of the CMB. A given theory, specified by some set of cosmic parameters, makes predictions about the distribution of the coefficients a^T_{lm}. For Gaussian theories like inflation, the coefficients are drawn from a normal distribution, with zero mean. In this case, all of the predictions of the theory are encoded in their variance. Therefore, the predictions of the theory can be written in terms of the C_l coefficients, defined by

$$C_{Tl} \equiv \left\langle a^T_{lm} \, a^{T*}_{lm} \right\rangle . \tag{5}$$

In general, the temperature anisotropy does not contain all of the information in the CMB because the CMB is polarized. The symmetric, trace-free polarization tensor $\mathcal{P}_{ab}$ can be decomposed into two kinds of scalar modes with opposite parities: an electric-type mode and a magnetic-type mode [41]. The polarization field can be expanded in terms of electric and magnetic type spherical harmonics $Y^{E,B}_{lm(ab)}$, with parity $(-1)^l$ and $(-1)^{l+1}$ respectively:

$$\frac{\mathcal{P}_{ab}(\theta,\phi)}{T_0} = \sum_{lm} \left[a^E_{lm} Y^E_{lm(ab)}(\theta,\phi) + a^B_{lm} Y^B_{lm(ab)}(\theta,\phi) \right] . \tag{6}$$

When polarization is included, the information in the CMB anisotropy can be characterized by three additional correlation functions

$$\begin{aligned} C_{El} &\equiv \left\langle a^E_{lm}\, a^{E*}_{lm} \right\rangle , \\ C_{Bl} &\equiv \left\langle a^B_{lm}\, a^{B*}_{lm} \right\rangle , \\ C_{Cl} &\equiv \left\langle a^T_{lm}\, a^{E*}_{lm} \right\rangle . \end{aligned} \tag{7}$$

Because the magnetic mode has parity opposite the temperature and electric modes, the $T-B$ and $E-B$ correlation functions vanish [42]. In this work we assume that the primordial perturbations are purely scalar density perturbations, with no tensor component. Their lack of handedness implies that scalar density perturbations cannot generate the magnetic-type modes [43]. Therefore $C_{Bl} = 0$ for the models we will consider. This assumption is motivated by the fact that most inflationary models produce tensor fluctuations too small to be easily detected, even with future satellite-based experiments [44]. In any case, for simplicity we will ignore this possibility.

The CMB anisotropy is related to perturbations to the photon distribution function, which is itself coupled to other particle species and gravitational metric perturbations through particle interactions and gravity. In this work we use the synchronous-gauge, where the coordinate and proper time of freely-falling observers coincide; all of the metric fluctuations occur in the spatial part of the metric, $ds^2 = a^2(\tau)\left[-d\tau^2 + (\delta_{ij} + h_{ij})\, dx^i dx^j\right]$. The metric perturbations h_{ij} can be decomposed into scalar, vector and tensor components; we will be concerned solely with the scalar perturbations. These can be written in terms of two scalar functions h and η [45]. In Fourier space,

$$h_{ij}(\vec{k},\tau) = \left\{ \hat{k}_i \hat{k}_j\, h(\vec{k},\tau) + \left[\hat{k}_i \hat{k}_j - 2\delta_{ij}\, \eta(\vec{k},\tau) \right] \right\} , \tag{8}$$

where $\vec{k}$ is the Fourier mode and τ is conformal time defined in terms of regular time t and the scale factor a by the relation $d\tau = dt/a$. To calculate the CMB anisotropy we need to know the metric perturbations h and η, as well as the distribution functions for all components: decaying neutrinos, decay radiation, photons, massless neutrinos and cold dark matter (CDM). The differences between a standard scenario with no decaying neutrinos, and the decaying neutrino scenarios we consider can be summarized as follows. In a decaying neutrino model:

- The energy densities of some of the components evolve differently from the standard case. This affects the dynamics of the expansion of the universe through the Friedmann equation, i.e., the Hubble parameter $\dot{a}/a$ is modified. This modification is covered in Secs. III A and III B.

- The Boltzmann equations that govern the evolution of the decaying neutrino and decay radiation perturbations must be modified to include decay terms. This is covered in Sec. III C.

A. Friedmann equation

The evolution of the scale factor is governed by the Friedmann equation. For the flat universes considered here,

$$\left(\frac{\dot{a}}{a}\right)^2 = \left(\frac{a}{a_0}\right)^2 \frac{8\pi}{3m_p^2}\rho(a) , \tag{9}$$

where $m_p = 1.221 \times 10^{22}$ MeV is the Plank mass and $\rho(a)$ is the total energy density. In this work, overdots are used to denote derivatives with respect to conformal time. The total density can be broken into components: the decaying neutrino ρ_h, its decay products ρ_{rd}, standard radiation ρ_{sr}, i.e., photons and two massless species of neutrinos, CDM + baryons ρ_m, and vacuum energy density ρ_Λ. The standard components evolve simply with scale factor: $\rho_{sr} \propto a^{-4}$, $\rho_m \propto a^{-3}$, $\rho_\Lambda \propto a^0$. However, decays (and possible inverse decays) complicate the decaying neutrino and decay product density evolution, which complicates the Friedmann equation and makes it impossible to solve analytically, except in special cases.

B. Energy density evolution equations

The distribution function for the i-th component, $f_i(x^j, q^j, \tau)$ depends in general on seven variables: position x^j, comoving momentum $q_i^j = a p_i^j$ where p_i is the proper momentum, and conformal time τ; it evolves according to the Boltzmann equation,

$$\frac{df_i}{d\tau} = \frac{\partial f_i}{\partial \tau} + \frac{dx^j}{d\tau}\frac{\partial f_i}{\partial x^j} + \frac{dn^j}{d\tau}\frac{\partial f_i}{\partial n^j} + \frac{dq}{d\tau}\frac{\partial f_i}{\partial q} = aC[f_i^0]\,, \tag{10}$$

where n^j is a normalized vector in the direction of the momentum, $q_i^j = q_i n^j$, and $C[f_i^0]$ is a collision functional that describes particle interactions. The factor of a multiplying the collision functional is just convention; it is a conversion between conformal time and real time, where collision terms are more easily described.

To find the equations governing the evolution of the energy densities, we consider the Boltzmann equation for the zeroth order distribution function, $f_i^0(q,\tau)$, denoted with a superscript-0. By zeroth order, we mean that we are neglecting the spatial perturbations in the distribution functions, so that the term proportional to $\partial f_i^0/\partial x^i = 0$. The quantity $dq/d\tau$ is first order in the metric perturbations [45], so that it too can be neglected. We also assume that f_i^0 does not depend on the momentum direction ($\partial f_i^0/\partial n^j = 0$), but allow f_i^0 to have arbitrary dependence on q_i. In this limit the Boltzmann equation simplifies:

$$\frac{\partial f_i^0}{\partial \tau} = aC[f_i^0]\,. \tag{11}$$

For the decay process $\nu_h \to \nu_l\,\phi$, the component i is either the decaying neutrino ($i \to h$) or one of the decay products ($i \to l$, or $i \to \phi$). We can find the zeroth-order energy density from the distribution function using the definition

$$\rho_i^0 = \frac{1}{a^4}\frac{g_i}{2\pi^2}\int_0^\infty dq\, q^2\, \epsilon\, f_i^0(q)\,, \tag{12}$$

where $\epsilon_i = \sqrt{q_i^2 + a^2 m_i^2}$ and g_i is the number of internal degrees of freedom for particle i. For the massive and massless neutrinos, $g_h = g_l = 2$, and for the scalar decay particle $g_\phi = 1$ since it is assumed to be spin-0 and its own antiparticle.

We next turn to the collision terms. In general, every type of interaction that the particle experiences will contribute to the these terms. Fortunately, in the case of decaying neutrinos, only a few interactions are important. Because the decaying neutrino interacts with the rest of the universe via the weak interaction, it decouples at a very high temperature of order a few MeV, just like standard, massless neutrinos. So for temperatures of interest here (eV-scale rather than MeV-scale), the decaying neutrino-decay radiation system is decoupled from the rest of the universe. Therefore, the only processes that are important are decays and inverse decays. Scatterings can be neglected in the calculation of energy densities, since they just shuffle energy among particles [19].

For the massive neutrino ($i \to h$) the collision functional can be written [19],

$$\begin{aligned}
C_h[f_h^0] &= -\Gamma_D^h + \Gamma_{ID}^h\,,\\
\Gamma_D^h &= \frac{1}{t_d}\frac{a\,m_h}{\epsilon_h\, q_h} f_h^0(q_h)\int_{1/2(\epsilon_h - q_h)}^{1/2(\epsilon_h+q_h)} dq_1\,\left[1 + f_\phi^0(q_1)\right]\left[1 - f_l^0(\epsilon_h - q_1)\right]\,,\\
\Gamma_{ID}^h &= \frac{1}{t_d}\frac{a\,m_h}{\epsilon_h\, q_h}\left[1 - f_h^0(q_h)\right]\int_{1/2(\epsilon_h - q_h)}^{1/2(\epsilon_h+q_h)} dq_1\, f_\phi^0(q_1) f_l^0(\epsilon_h - q_1)\,.
\end{aligned} \tag{13}$$

In this expression Γ_D^h arises from decays, $\nu_h \to \nu_l\phi$ and Γ_{ID}^h arises from inverse decays, $\nu_l\phi \to \nu_h$. The integration limits follow from the kinematics of the interactions.

The collision terms for the decay products are similar to those for the decaying neutrino. For the light neutrino ($i \to l$),

$$\begin{aligned}
C_l[f_l^0] &= -\Gamma_D^l + \Gamma_{ID}^l\,,\\
\Gamma_D^l &= \frac{1}{t_d}\frac{a\,m_h}{q_l^2}\left[1 - f_l^0(q_l)\right]\int_{a^2 m_h^2/4q_l^2}^{\infty} dq_\phi\,\left[1 + f_\phi^0(q_\phi)\right] f_h^0\left(\sqrt{(q_\phi + q_l)^2 - a^2\, m_h^2}\right)\,,\\
\Gamma_{ID}^l &= \frac{1}{t_d}\frac{a\,m_h}{q_l^2} f_l^0(q_l)\int_{a^2 m_h^2/4q_l^2}^{\infty} dq_\phi\, f_\phi^0(q_\phi)\left[1 - f_h^0\left(\sqrt{(q_\phi + q_l)^2 - a^2\, m_h^2}\right)\right]\,,
\end{aligned} \tag{14}$$

and, for the scalar particle ($i \rightarrow \phi$),

$$
\begin{aligned}
C_\phi[f^0_\phi] &= -\Gamma^\phi_D + \Gamma^\phi_{ID}\,, \\
\Gamma^\phi_D &= 2\frac{1}{t_d}\frac{a\,m_h}{q^2_\phi}\left[1+f^0_\phi(q_l)\right]\int_{a^2m^2_h/4q^2_\phi}^\infty dq_l\,\left[1+f^0_\phi(q_\phi)\right] f^0_h\left(\sqrt{(q_l+q_\phi)^2-a^2\,m^2_h}\right)\,, \\
\Gamma^l_{ID} &= 2\frac{1}{t_d}\frac{a\,m_h}{q^2_\phi} f^0_\phi(q_\phi)\int_{a^2m^2_h/4q^2_\phi}^\infty dq_l\, f^0_l(q_l)\left[1-f^0_h(\sqrt{(q_\phi+q_l)^2-a^2\,m^2_h})\right]\,.
\end{aligned}
\tag{15}
$$

The Boltzmann equation for each type of particle, Eq. 11, their collision term equations, Eqns. 13–15, and the Freidman equation, Eq. 9, determine the dynamics of the expansion of the universe. They form a closed set of integro-differential equations for the evolution of the scale factor, and require numerical methods for their solution. In particular, the collision term integrals are complicated functions of momentum. However, for certain special cases these equations simplify, and for other cases we can estimate the late-time densities without having to solve the equations at all.

1. *Out-of-equilibrium decays*

Neutrino decays become important when the age of the universe is near the neutrino mean lifetime. If $T(t_d) \ll m_h/3$, where $T(t_d)$ is the temperature of the universe at time t_d after the big-bang, the neutrino decays non-relativistically, so that when the neutrino starts to decay, the thermal energy of the decay products cannot overcome the rest mass energy of the decaying neutrinos. This suppresses inverse decays relative to decays and causes the decays to occur out of equilibrium. We will use the terms out-of-equilibrium decays and non-relativistic decays interchangeably. Thus, the neutrino decays away when $t \sim t_d$. These decays can generate a large amount of decay radiation, depending on the initial abundance of the decaying neutrino and how non-relativistic the neutrino is at decay.

Since neutrinos decouple from the rest of the universe at a very high temperature determined by their weak interactions, all of the neutrinos, including the massive, decaying neutrino, are ultra-relativistic at decoupling (we will not consider MeV-scale decaying neutrinos). Thus, their abundances are large, of order the photon abundance. The decaying neutrino, if still present, becomes non-relativistic when $T \lesssim m_h/3$. Then its energy density scales as matter, as a^{-3} instead of as radiation, which scales as a^{-4}. Its energy density, and consequently the energy density of its decay products, becomes relatively more important the longer the decaying neutrino is still around and non-relativistic.

For out-of-equilibrium decays, simplified evolution equations for the decaying neutrino and decay radiation densities can be found. The collision term for the decaying neutrino simplifies, because in this limit we can neglect f^0_l and f^0_ϕ:

$$
C_h[f^0_h] \simeq \frac{q}{t_d}\,\frac{m_h}{\epsilon_h}\,f^0_h\,. \tag{16}
$$

The Boltzmann equation can then be converted into a differential equation for ρ^0_h, by multiplying each term by $p^2_h E_h$ and integrating out p_h. We find that

$$
\frac{\partial \rho^0_h}{\partial \tau} + 3\frac{\dot a}{a}\left(\rho^0_h + P^0_h\right) = -\frac{a m_h}{t_d}\,n^0_h\,, \tag{17}
$$

where P^0_h is the pressure and n^0_h is the number density of the decaying neutrinos, given by the definitions,

$$
\begin{aligned}
n^0_i &= \frac{1}{a^3}\frac{g_i}{2\pi^2}\int_0^\infty dq\,q^2\,f^0_i(q)\,, \\
P^0_i &= \frac{1}{a^4}\frac{g_i}{2\pi^2}\int_0^\infty dq\,\frac{q^4}{3\epsilon}\,f^0_i(q)\,.
\end{aligned}
\tag{18}
$$

A couple of comments about the evolution equation for ρ^0_h are in order. Note the presence of a pressure term P^0_h on the left hand side. In the limit of completely non-relativistic decays, this term is zero, but otherwise this term can be a significant correction. If we neglect the pressure term, then the $3(\dot a/a)\rho_h$ term represents the fact that matter density varies as a^{-3} in the absence of decays. A similar comment applies to the product $m_h\,n^0_h$ on the left hand side. For completely non-relativistic decays, all of the decaying neutrino energy is rest mass energy so that $m_h\,n^0_h = \rho^0_h$, but otherwise the two quantities are not equal.

Given the decaying neutrino energy density, the decay product energy density $\rho_{rd} = \rho_l + \rho_\phi$ can be obtained from the first law of thermodynamics [46]:

$$\frac{d(a^3\rho_{rd})}{d\tau} = -P_{rd}\frac{da^3}{d\tau} - \frac{d(a^3\rho_h)}{d\tau}\,. \tag{19}$$

Since the decay radiation is massless, $P_{rd} = 1/3\rho_{rd}$, and we find that

$$\frac{d\rho_{rd}}{d\tau} + 4\frac{\dot{a}}{a}\rho_{rd} = -\left(\frac{d\rho_h}{d\tau} + 3\frac{\dot{a}}{a}\rho_h\right) = -\frac{a}{t_d}\rho_h\,, \tag{20}$$

where the second equality holds for fully non-relativistic decays. In the absence of decays, this equation implies that the decay radiation density scales as a^{-4}, as expected for massless particles. Finally, we can obtain a simpler equation, which will be useful later, for the evolution of the decay radiation density. Let $r_{rd} = \rho^0_{rd}/\rho^0_{1\nu}$, where $\rho^0_{1\nu}$ is the density in a single species of standard, massless neutrinos. Then Eq. 20, and the fact that $\rho^0_{1\nu} \propto a^{-4}$, implies that

$$\frac{dr_{rd}}{d\tau} = \frac{m_h\, n^0_h}{\rho_{1\nu}}\,\frac{a}{t_d}\,. \tag{21}$$

To find the energy densities of the decaying neutrino and its decay radiation for out-of-equilibrium decays, we numerically solve Eqns. 17 and 20, together with the Friedmann equation, Eq. 9 [56]. Results for several decaying neutrino models are shown in Fig's 1 and 2. There we plot the energy densities, scaled by the critical density, for all of the components: standard radiation, CDM, vacuum energy density, decaying neutrino and decay radiation. The first figure shows a succession of masses with lifetimes fixed at 10^9 sec. These are models where the neutrino decays before last scattering, $t_{rec} \sim 10^{13}$ sec. It is easy to see that the decay radiation becomes more important as the mass increases, in keeping with Eq. 23. If the neutrino is massive enough, then it can cause an early phase of matter domination before it decays and its decay radiation dominates. The second figure shows some models where the neutrino decays after last scattering.

By determining how non-relativistic the neutrino is when it decays, it is possible to obtain an estimate of the energy density in decay radiation, without resorting to the full Boltzmann equations. To do this we define a relativity parameter α, proportional to the square of the decaying neutrino's mass divided by its thermal energy at the time of decay, and with the property that $\alpha \simeq 1$ at the border between relativistic and non-relativistic decays. For non-relativistic decays, $\alpha \gg 1$ and $\rho_{rd}/\rho_{1\nu}$ is large; for ultra-relativistic decays, $\alpha \ll 1$ and $\rho_{rd}/\rho_{1\nu} \simeq 1$. Consider a scenario with $\alpha \simeq 1$. Here, the universe is never dominated by the massive neutrino. For a radiation dominated universe at decay, the Friedmann equation gives the relation between decay time and temperature [46], $t_d \simeq 0.3 g_*^{-1/2} m_p/T_d^2$, where $g_* \simeq 3.36$ is the effective number of relativistic degrees of freedom. Since the temperature at decay $T_d \simeq m_h/3$, the neutrino parameters enter in the combination $m_h^2 t_d$, which implies that

$$\alpha = 0.11\left(\frac{m_h}{\mathrm{MeV}}\right)^2\left(\frac{t_d}{\mathrm{sec}}\right)\,. \tag{22}$$

Because matter density decreases as one power of the scale factor relative to radiation density, we can estimate the energy density in decay radiation in units of standard massless neutrinos, N_{rd}, as follows: $N_{rd} \simeq a_d/a_{nr}$, where a_{nr} is the scale factor when the neutrino becomes non-relativistic and a_d is the scale factor at decay. Here we assume that the decay instantaneously transforms the density in decaying neutrinos to the decay radiation. If the universe is dominated by the decaying neutrino at decay, then the Friedmann equation can be used to obtain a_d. The result is that [31]

$$N_{rd} \simeq 0.52\,\alpha^{2/3}\,, \tag{23}$$

valid for $\alpha \gg 1$. The numerical coefficients in Eqns. 22 and 23, but not the overall dependence, have been fudged by a small amount so that the the formula for N_{rd} agrees well with numerical results. The bottom pane of Fig. 3 shows this estimate versus numerical results for the total radiation density $N_\nu = N_{rd} + 2$, as a function of α. The 2 represents the two species of massless neutrinos. As the figure shows, the agreement is good as a rough estimate.

2. Equilibrium decays

If $T(t_d) \gg m_h/3$, neutrino decays become important while the neutrino is still ultra-relativistic. In this case both decays and inverse decays occur, and the collision terms do not simplify. It is, however, possible to obtain an estimate

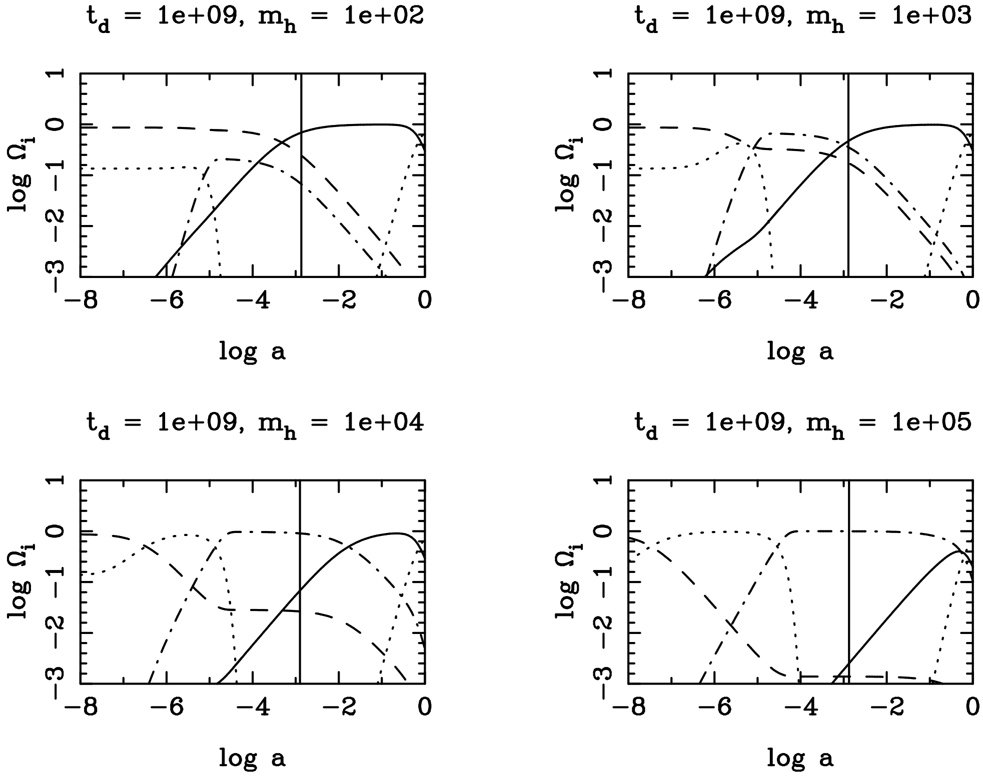

FIG. 1: The evolution of the energy densities, relative to the critical density, of the various components of the universe, in early-decaying scenarios. The notation is as follows: solid line = CDM+baryons, long-dashed line = standard radiation (photons + 2 massless neutrinos), dotted line = decaying neutrino, dot-dashed line = decay radiation. For all values of the scale factor, $\sum_i \Omega_i = 1$. The background cosmological model has a cosmological constant $\Omega_\Lambda = 0.7$ today. The vertical line represents the epoch of recombination. The models shown here all have $t_d = 10^9$ sec; m_h varies from 10^2 to 10^5 eV. For $m_h = 10^2$ eV, the decay is barely non-relativistic: $\alpha = 1.1$. The decay radiation density never matches the density in standard radiation. For the higher-mass scenarios, the decays are out-of-equilibrium and the decay radiation dominates the standard radiation for all times after decay. Another feature to be noted is the relative importance of components at recombination; this determines the amount of the early-ISW effect. For $m_h = 10^4$, 10^5 eV, the universe is radiation dominated at last scattering, creating a large early-ISW effect.

for the energy density in decay products long after the neutrino has decayed away. This estimate relies on the fact that when $t \gtrsim t_d$, the decay and inverse decay processes are sufficiently fast relative to the expansion rate to establish chemical equilibrium between the decaying neutrino and its decay products [22]. Then the distribution functions are approximately thermal in form with pseudo-temperature T' not necessarily equal to the temperature of the universe. Therefore, we have

$$f_i^0 = \frac{1}{e^{(E_i - \mu_i)/T'} \pm 1}\,, \tag{24}$$

for $i = h$, l, or ϕ, with pseudo-chemical potentials related by

$$\mu_h = \mu_l + \mu_\phi\,. \tag{25}$$

It is easy to show that the Boltzmann equations imply that the following relations hold generally [19]:

$$\frac{d}{d\tau}\left(a^3\left(n_h + n_l\right)\right) = 0\,, \tag{26}$$

$$\frac{d}{d\tau}\left(a^3\left(n_h + n_\phi\right)\right) = 0\,, \tag{27}$$

and that for $T \gg m_h$, the following holds:

$$\frac{d}{d\tau}\left(a^4\left(\rho_h + \rho_l + \rho_\phi\right)\right) = 0\,. \tag{28}$$

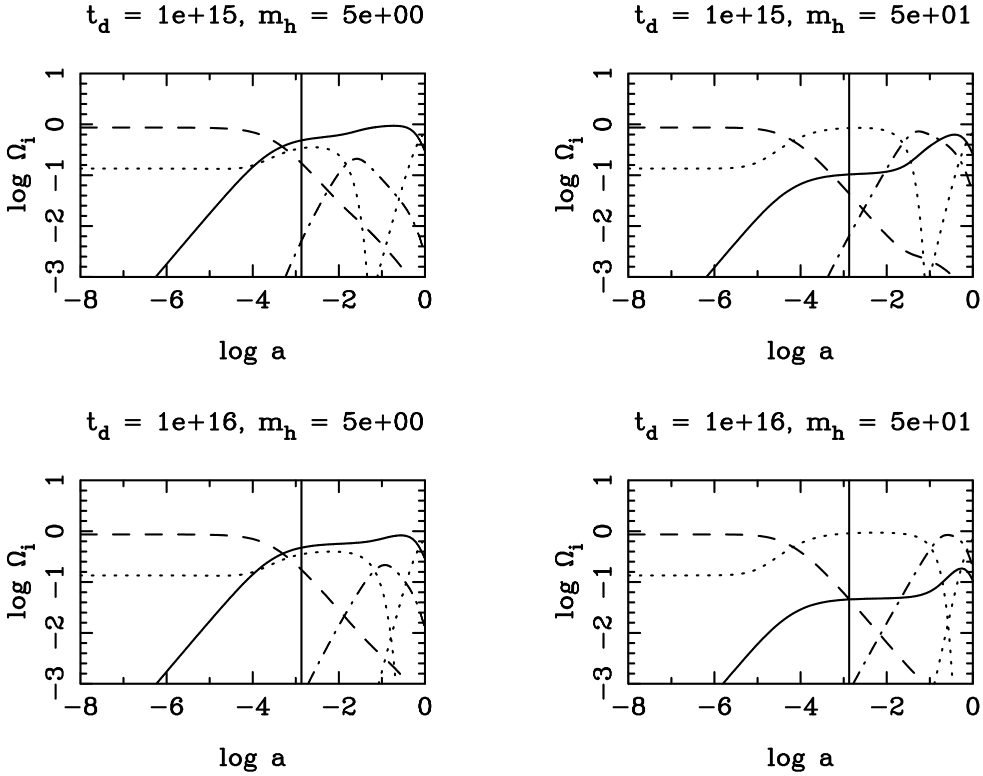

FIG. 2: Same as Fig. 1, but for late-decaying neutrinos. In neither $m_h = 5$ eV scenario does either the massive neutrino or its decay products ever dominate the energy density. In both scenarios with $m_h = 50$ eV, the universe is dominated by the massive neutrino at recombination, and by the decay radiation at decay.

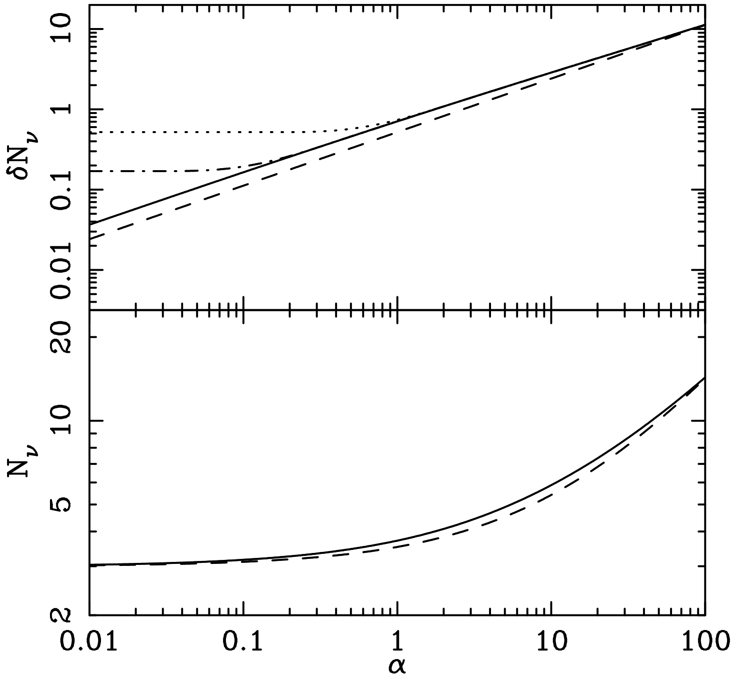

FIG. 3: Late-time asymptotic behavior of extra radiation energy density expressed in units of species of massless neutrinos, as a function of relativity parameter α. Plotted are the non-equilibrium limit $\delta N_\nu = 0.52\alpha^{3/2}$, valid for $\alpha \gg 1$, as well as data for 2-body decays ($\nu_h \to \nu_l\, \phi$) and 3-body decays ($\nu_h \to \nu_l\, \nu_l\, \nu_l$). In both the 2 and 3-body decay scenarios we have assumed an initial thermal abundance of heavy and light neutrinos at the standard neutrino temperature $T_\nu = (4/11)^{1/3} T_\gamma$.

This equation implies that the total comoving energy density in the decaying neutrino-decay radiation system is unchanged by the decay/inverse decay processes, for $T(t_d) \gg m_h$.

We numerically solve Eqns. 25, 26, 27, and 28 for μ_h, μ_l, μ_ϕ, and T'. For initial conditions we assume a thermal initial abundance of heavy and light neutrinos, and no initial scalar particles. We find that

$$\mu_h = 0.092\, T_\nu\,,\ \mu_l = 0.581\, T_\nu\,,\ \mu_\phi = -0.489\, T_\nu\,,\ T' = 0.884\, T_\nu\,, \tag{29}$$

where $T_\nu = (4/11)^{1/3} T$ is the standard neutrino temperature. This solution if valid for $t \gtrsim t_d$ and $m_h \lesssim T(t)$. When the universe cools enough so that $T \lesssim m_h/3$, the inverse decays become suppressed and decays predominate. The rest mass of the heavy neutrinos is starting to become important, increasing their total energy relative to the massless case. As they decay away, the energy density in heavy neutrinos is then transferred to the decay radiation, raising its temperature. We can calculate the amount of heating by using the fact that the entropy of the heavy neutrino-decay radiation system is conserved. We find that the neutrino decays raise the decay radiation temperature by 14.7%. Our final result, the energy density in decay radiation, can be expressed in units of standard, massless neutrino energy density: $N_{rd} = 2.17$. In a scenario with no decaying neutrinos, this number would be 2.0, so $\delta N_\nu = 0.17$, where δN_ν is the change in radiation density. A similar procedure could also be repeated for the case of three body decays: $\nu_h \to 3\,\nu_l$. In this case, $\delta N_\nu = 0.52$ for $\alpha \ll 1$, and the large-α behavior of the radiation density is identical to the two-body case.

Results for the decay radiation energy density, for both equilibrium and out-of-equilibrium decays, are shown in Fig. 3. To summarize, for $T(t_d) \ll m_h/3$, decays occur in equilibrium, with decays and inverse decays important for $t \gtrsim t_d$. For $t_d < t < t(T = m_h/3)$ the energy density in radiation is repartitioned, but the total value is the same as if the neutrino did not decay. For $t \gtrsim t(T = m_h/3)$, the heavy neutrino decays away and increases the total radiation density by 2.3%.

C. Perturbation Boltzmann equations

Following reference [45], we would like to derive a hierarchy of Boltzmann equations describing the evolution of perturbations to the decaying neutrinos and the decay radiation. The i-th distribution function can be written as the product of an unperturbed, thermal function times a perturbation, as follows:

$$f_i(x^j, q, n^j, \tau) = f_i^0(q,\tau)\left[1 \pm \Psi_i(x^j, q, n^j, \tau)\right]\,. \tag{30}$$

The Boltzmann equation, Eq. 10, then yields an equation for the evolution of the perturbation. Upon taking the Fourier transform,

$$\frac{\partial \Psi_i}{\partial \tau} + i\frac{q_i}{\epsilon_i}\left(\vec{k}\cdot\vec{n}\right)\Psi_i + \frac{d\ln f_i}{d\ln q_i}\left[\dot{\eta} - \frac{1}{2}(\dot{h}+\dot{\eta})(\vec{k}\cdot\vec{n})^2\right] = \frac{1}{f_i^0}\left(\frac{\partial f}{\partial \tau}\right)_C\,. \tag{31}$$

Since the decay radiation is effectively massless, $\epsilon_{rd} = q_{rd}$, and we can integrate the momentum dependence out of the Boltzmann equation. We define a momentum-independent perturbation F_{rd} as in reference [45], scaling it by the decay related factor r_{rd} for convenience:

$$F_{rd}(\vec{k},\hat{n},\tau) \equiv \frac{\int dq\, q^3 f_{rd}^0(q,\tau)\Psi_{rd}(\vec{k},q,\hat{n},\tau)}{\int dq\, q^3 f_{rd}^0(q,\tau)}\, r_{rd}\,. \tag{32}$$

Unfortunately, the complicated form for the collision terms in the Boltzmann equation makes it difficult to derive simple equations in the general case. *For the rest of this section, we will specialize to the case of out-of-equilibrium decays*, where these terms simplify. Then the Boltzmann equation governing F_{rd} can be shown to be [32]

$$\dot{F}_{rd} + \imath k\mu F_{rd} + 4\left(\frac{\dot{h}}{6} + \frac{\dot{h}+6\dot{\eta}}{3}P_2(\mu)\right) r_{rd} = \dot{r}_{rd} N_0\,, \tag{33}$$

where

$$N_0(k,\tau) = \frac{\int dq_h\, q_h^2 f_h^0(q_h,\tau)\Psi_h(k,q_h,\tau)\left[1 - \frac{8}{3}\left(\frac{q_h}{a m_h}\right)^2\right]}{\int dq_h\, q_h^2 f_h^0(q_h,\tau)}\,, \tag{34}$$

$\mu = \hat{k}\cdot\hat{n}$ and $P_n(\mu)$ are the Legendre polynomials of order n. In Eqns. 33 and 34, only terms up to $\mathcal{O}(q_h^2/a^2m_h^2)$ have been kept. Similar equations for the evolution of perturbations in the decay radiation can be found in references [26], [28] and [32].

The dependence of F_{rd} on μ can be eliminated by expressing it as a series of Legendre polynomials, $F_{rd} = \sum_l F_{rd,l}\,P_l$, leading to the following Boltzmann hierarchy for the decaying neutrino perturbations, valid for out-of-equilibrium decays:

$$\begin{aligned}
\dot{\delta}_{rd} &= -\frac{2}{3}\left(\dot{h}+2\theta_{rd}\right) - \frac{\dot{r}_{rd}}{r_{rd}}\left(\delta_{rd}-\delta_h\right)\,, \\
\dot{\theta}_{rd} &= k^2\left(\frac{1}{4}\delta_{rd}-\sigma_{rd}\right) - \frac{\dot{r}_{rd}}{r_{rd}}\theta_{rd}\,, \\
\dot{\sigma}_{rd} &= \frac{2}{15}\left(2\theta_{rd}+\dot{h}+6\dot{\eta}\right) - \frac{\dot{r}_{rd}}{r_{rd}}\sigma_{rd}\,, \\
\dot{F}_{rd,l} &= \frac{k}{2l+1}\left[lF_{rd,l-1}-(l+1)F_{rd,l+1}\right] - \frac{\dot{r}_{rd}}{r_{rd}}F_{rd,l}\,,\quad l\geq 3
\end{aligned} \tag{35}$$

where $\delta_{rd} = F_{rd,0}/r_{rd}$, $\theta_{rd} = 3kF_{rd,1}/4r_{rd}$ and $\sigma_{rd} = F_{rd,2}/2r_{rd}$. This set of equations is identical to the Boltzmann hierarchy for standard massless neutrinos, with the addition of the terms proportional to $\dot{r}_{rd}/r_{rd} \propto 1/t_d$. The extra decay term can have a large effect on the decay radiation perturbations when $t \sim t_d$, but for late times the perturbations approach the values they would have attained in its absence. To calculate the decay radiation perturbations, we added a separate Boltzmann hierarchy, described by Eq. 35. In our numerical scheme, this hierarchy must be terminated at some value of multipole moment l_{end}. We terminate the hierarchy by adding the extra equation for $F_{rd,l_{end}+1}$,

$$F_{rd,l_{end}+1} = \frac{2l_{end}+1}{k\tau}F_{rd,l_{end}} - F_{rd,l_{end}-1}\,, \tag{36}$$

the method used for the massless neutrino hierarchy in CMBFAST [47].

Because the decaying neutrinos are massive, $\epsilon_h \neq q_h$, and it is impossible to integrate the momentum dependence from their perturbations. After expanding the decaying neutrino perturbation in terms of Legendre polynomials, $\Psi_h = \sum_l \Psi_{h,l}P_l$, the Boltzmann equation becomes

$$\begin{aligned}
\dot{\Psi}_{h,0} &= -\frac{q_h k}{\epsilon_h}\Psi_{h,1} + \frac{1}{6}\dot{h}\frac{d\ln f_h}{d\ln q_h} - \frac{am_h}{t_d\epsilon_h}\Psi_{h,0}\,, \\
\dot{\Psi}_{h,1} &= \frac{q_h k}{3\epsilon_h}\left(\Psi_{h,0}-2\Psi_{h,2}\right) - \frac{am_h}{t_d\epsilon_h}\Psi_{h,1}\,, \\
\dot{\Psi}_{h,2} &= \frac{q_h k}{5\epsilon_h}\left(2\Psi_{h,1}-3\Psi_{h,3}\right) - \left(\frac{1}{15}\dot{h}+\frac{2}{5}\dot{\eta}\right)\frac{d\ln f_h}{d\ln q_h} - \frac{am_h}{t_d\epsilon_h}\Psi_{h,2}\,, \\
\dot{\Psi}_{h,l} &= \frac{q_h k}{\epsilon+h\,(2l+1)}\left[l\Psi_{h,l-1}-(l+1)\Psi_{h,l+1}\right] - \frac{am_h}{t_d\epsilon_h}\Psi_{h,l}\,,\quad l\geq 3\,.
\end{aligned} \tag{37}$$

This set of equations differs from the evolution equations for massive, non-decaying neutrinos only through the presence of the term proportional to $1/t_d$. The decay term is easily interpreted. For non-relativistic neutrinos, the m_h in the numerator cancels the ϵ_h in the denominator; the result is just the differential equation for exponential decay, in conformal time. If the neutrinos are not completely non-relativistic, then their velocities become important, and there is a time dilation factor associated with transforming between the neutrino rest frame and the thermal frame. In this case, m_h/ϵ_h becomes the special relativistic gamma factor for this transformation.

It should be noted that, for out-of-equilibrium decays, the perturbation evolution equations are independent of the details of the decay radiation, except for the fact that is must be light and weakly-interacting. The energy density equations, Eq. 20 and 17, are also independent of the details. Therefore, the CMB anisotropy becomes a function of m_h and t_d, independent of the decay channel. In fact, the calculations can be generalized to encompass generic decaying particles. The main difference in the generic scenario will be due to the initial abundance of the decaying particle which will depend on its interactions. However, a generic decaying particle will produce a CMB spectrum very similar to a decaying neutrino with the same lifetime, provided that the densities of decay radiation are the same. Finally, note that this simplification is valid for out-of-equilibrium decays only.

IV. ANALYZING THE DATA

This section briefly reviews estimating cosmic parameter uncertainties ("error forecasting"), and using data to rule out decaying neutrino parameter space. For further discussion of error forecasting in parameter estimation, see e.g., Refs. [42, 48, 49, 50, 51, 52]. The formalism used to determine which decaying neutrino models can be ruled out is discussed in the Appendix.

A. Measuring m_h and t_d

A given theory, specified by a set of cosmological parameters $\{\lambda_i\}$ ($i = 1 \ldots N$, with N the number of cosmic parameters considered) makes predictions about the multipole amplitudes, the C_l's. The results of a CMB experiment are estimates of the C_l's, with some experimental uncertainties. Of course, we cannot know in advance the values of C_l's that a given experiment will measure; however, by knowing what we expect for the uncertainties, we can estimate how large the uncertainties in the parameters should be.

For an experiment with data out to some maximum $l = l_{max}$, we can define a goodness of fit statistic that is a function of $\{\lambda_i\}$:

$$\chi^2(\{\lambda_i\}) = \sum_{l=2}^{l_{max}} \sum_{X,Y=T,E,C} \left[C_{Xl}^{theory}(\{\lambda_i\}) - C_{Xl}^{data}\right] V_{XYl}^{-1} \left[C_{Yl}^{theory}(\{\lambda_i\}) - C_{Yl}^{data}\right] , \tag{38}$$

where C_{Xl}^{theory} is the theoretical spectrum for cosmic parameters $\{\lambda_i\}$, C_{Xl}^{data} is the measured spectrum and V_{XYl} is the covariance matrix between estimators of the different spectra. For a cosmic variance limited experiment with data to some maximum $l = l_{max}$, the diagonal components of V_{XYl} are given by [42]

$$\begin{aligned} V_{TTl} &= \frac{2}{2l+1} C_{Tl}^2 , \\ V_{EEl} &= \frac{2}{2l+1} C_{El}^2 , \\ V_{CCl} &= \frac{2}{2l+1} \left(C_{Cl}^2 + C_{Tl} C_{El}\right) , \end{aligned} \tag{39}$$

and the non-zero off-diagonal components are given by

$$\begin{aligned} V_{TEl} &= \frac{2}{2l+1} C_{Cl}^2 , \\ V_{TCl} &= \frac{2}{2l+1} C_{Tl} C_{Cl} , \\ V_{ECl} &= \frac{2}{2l+1} C_{El} C_{Cl} , \end{aligned} \tag{40}$$

for $l \leq l_{max}$.

The measured cosmic parameters, $\{\lambda_i'\}$, are determined by minimizing $\chi^2(\{\lambda_i\})$:

$$\frac{\partial \chi^2_{min}}{\partial \lambda_j}(\{\lambda_i'\}) = 0 , \tag{41}$$

for $j = 1 \ldots N$. If we assume that the measured cosmic parameters are close to their actual values, denoted $\{\tilde{\lambda}_i\}$, then χ^2 can be expanded about its minimum as follows:

$$\chi^2\left(\{\lambda_i\}\right) \simeq \chi^2(\left\{\tilde{\lambda}_i\right\}) + \sum_{ij} \left(\lambda_i - \tilde{\lambda}_i\right) \alpha_{ij} \left(\lambda_j - \tilde{\lambda}_j\right) , \tag{42}$$

where α_{jk} is the Fisher matrix,

$$\alpha_{ij} = \sum_l \sum_{XY} \frac{\partial C_{Xl}^{theory}}{\partial \lambda_i} V_{XYl}^{-1} \frac{\partial C_{Yl}^{theory}}{\partial \lambda_j} . \tag{43}$$

The Fisher matrix determines how rapidly χ^2 increases as the cosmic parameters are varied away from their true values. Under certain reasonable assumptions [53], the uncertainties on the parameters are determined by this matrix. If we allow all cosmic parameters to vary simultaneously, then

$$\delta\lambda_i = \sqrt{(\alpha^{-1})_{ii}} . \tag{44}$$

The formalism above assumes data for both temperature and polarization. If only temperature data is obtained, then the covariance matrix V_{XYl} becomes a number:

$$V_{XYl} = \frac{2C_{Tl}^2}{2l+1}\, \delta_{XT}\, \delta_{YT}\,, \tag{45}$$

where δ is the discrete delta function.

To calculate the uncertainties in the parameters, we will assume some decaying neutrino scenario. The set of cosmic parameters will include neutrino parameters, like m_h and t_d. The uncertainties will then depend on the model we assume and the parameters we allow to vary.

B. Ruling out models

It could also be the case that no theoretical model can specify the data. For instance, in a decaying neutrino scenario, the data could be analyzed without considering neutrino parameters. In general, two things will then happen. 1) The best-fit parameters will be systematically offset from the true parameters. 2) No theoretical model will fit the data well, i.e., the best-fit χ^2 will be higher than expected. In special cases, one or the other thing will happen. For instance, if the effects on the CMB of the decaying neutrinos and their decay radiation is exactly mimicked by some perturbation to the set of cosmic parameters, then a ΛCDM model with offset parameters will fit the data well. If, on the other hand, the effects of the decaying neutrinos and the decay radiation are orthogonal to the effects of parameter offsets, then the offsets will be small, but no model will fit the data well. If no ΛCDM model can reproduce a decaying neutrino model, in the sense that the best-fit χ^2 is large, then the decaying neutrino model is said to be distinguishable from ΛCDM.

If the offsets are small, then the problem can be analyzed analytically. This is done in Appendix VII. The procedure we use to determine the distinguishability of a model is to calculate the C_l spectrum and the Fisher matrix for the cosmic parameters being considered, for the baseline ΛCDM model. Then, for a given decaying neutrino model we

- Find the parameter offsets using Eq. 52.
- Determine the probability distribution for the goodness of fit χ^2. Being approximately Gaussian, this distribution is fully characterized by expected the best-fit $\langle\chi^2_{min}\rangle$, given by Eq. 38 and the variance σ_χ, given by Eq. 65.
- Determine the level of distinguishability by convolving the probability distribution for χ^2_{min} with the allowed level for each χ^2_{min}, as per Eq. 66.

V. REGIONS OF PARAMETER SPACE

In decaying neutrino scenarios, the physics of the neutrino decays, and therefore the CMB anisotropy changes as the neutrino parameters are varied. It is therefore useful to break the parameter space into regions and consider each region separately. To do so we first note that several physical scales naturally divide the parameter space:

- $t_d = t_U$: This represents the division between stable and unstable neutrinos.
- $\Omega_0 h^2 = 0.25$: For our decaying neutrino models, we let Ω_{CDM} vary to enforce a flat universe: $\Omega_0 = 1$. If the density in neutrinos or decay radiation today is large enough, then $\Omega_0 > 1$ even with no CDM. For reasonable values of h_0, regions with $\Omega_0 > 1$ tend to produce universes young enough to violate independent age constraints: $\Omega_0 h^2 < 0.25$. For stable neutrinos, this translates into the well-known bound on the sum of the masses, $\sum_i m_i \leq 24$ eV, where the index i runs over all neutrino species.
- $t_d = t_{rec}$: The decay radiation for neutrinos that decay before last scattering sources CMB anisotropy through early-ISW effect, while the decay radiation for neutrinos that decay after last scattering creates a late-ISW effect.
- $m_h = 3T(t_d)$: This scale divides equilibrium ($m_h \lesssim 3T(t_d)$) from out-of-equilibrium ($m_h \gtrsim 3T(t_d)$) decaying neutrinos. Neutrinos that decay in equilibrium produce small changes in the radiation density, while those that decay out-of-equilibrium produce larger effects.
- $m_h = 3T(t_{rec})$: This scale determines whether the decaying neutrinos are relativistic ($m_h \lesssim 3T(t_{rec})$ or non-relativistic ($m_h \gtrsim 3T(t_{rec})$ at last scattering.

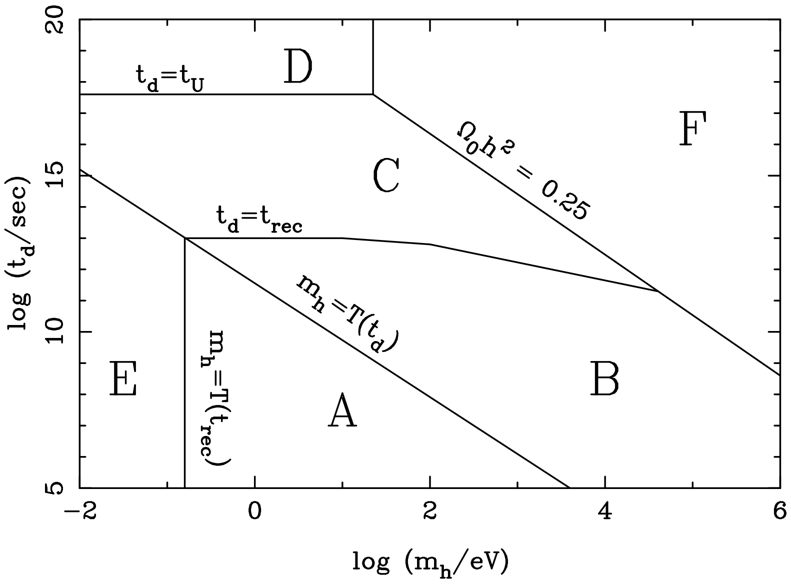

FIG. 4: Decaying neutrino parameter space, divided into regions according to the physics of the CMB anisotropy.

Based on these scales, we have broken the decaying neutrino parameter space into regions, labeled alphabetically, as shown in Fig. 4:

- A: $3T(t_{rec}) < m_h < 3T(t_d)$

  In this region the neutrino decays in equilibrium, before last scattering. The energy density in radiation is increased relative to the standard case by $\delta N_\nu = 0.17$. The only difference between the CMB anisotropy of these models and the baseline model is due to this extra radiation. If the universe is not completely matter-dominated at last scattering, then the gravitational potentials are decaying at last scattering, when the primary anisotropy is being formed. Decaying potentials at last scattering generate anisotropy through the early-ISW effect. The small amount of extra radiation in these models induces a small amount of extra anisotropy. The angular scale of the effect is determined by the sound horizon at last scattering, placing the feature near the first acoustic peak, which, for the flat universes that we consider, $l \sim 200$. The degeneracy in m_h and t_d means that these models can be considered as a group.

  Because the CMB anisotropy in this region depends only on the radiation density at last scattering, the details of the decay channel are unimportant, except to the extent that they determine this density. For example, it is easy to extend the analysis to include the three-body decay scenario $\nu_h \to \nu_l\, \nu_l\, \nu_l$, because we know that in this scenario, $\delta N_\nu = 0.52$.

  The claim that we can calculate the CMB spectrum for models in region-A by simply adding 0.17 species of massless neutrinos bears examination. One possible concern follows from the fact that if massive neutrinos are present near last scattering, then they will affect the CMB anisotropy. However, in this region there are no massive neutrinos left at last scattering; they have decayed away by then. A more serious concern involves spatial perturbations to the decay radiation. Treating the decaying radiation by simply increasing the effective number of massless neutrino species effectively assumes that the decay radiation perturbations are equal to massless neutrino perturbations. But for times much later than those when decays are important, the decay radiation perturbations approach those for massless neutrinos. This is because the collision term in the Boltzmann equation that describes the perturbation evolution, described in Sec. III C, is only important when decays are important, and the evolution equations without the collision term are identical to those for standard massless neutrinos. In this region, the decaying neutrinos decay away when they become non-relativistic, when $T(t) \lesssim m_h/3$. If this time is much earlier than recombination, i.e., if $m_h \ll 3T(t_{rec})$, then the decay radiation perturbations can be approximated as standard massless neutrinos, and the arguments in the last paragraph hold. From Fig. 4, this condition holds in region-A, for points a good deal to the right of the defining line $m_h = 3T(t_{rec})$. We will assume that this is true for the rest of this work.

- B: $m_h > 3T(t_d)$, $t_d < t_{rec}$

  Here, neutrinos decay out-of-equilibrium, before last scattering. Thus, as for region-A, the decay radiation sources the early-ISW effect which results in extra anisotropy near the first acoustic peak. But the effects are larger in this region since out-of-equilibrium decays can generate large amounts of decay radiation, as shown in Eq. 23. The amount of extra radiation, and hence the CMB spectrum, depends on one parameter only, either α or δN_ν. This is in contrast this to the constant effect in region-A. Some models from region B, parameterized by δN_ν, are shown in Fig. 5. Another effect is visible in addition to the early-ISW acoustic peak enhancement: a shift of all features to smaller angular scales. This is due to the fact that, as the amount of radiation at last scattering increases, the sound horizon at last scattering decreases. For the standard ΛCDM model, the universe is mostly matter-dominated at last scattering, with $\tau = 2\sqrt{a}H_0^{-1}$. In the limit of a completely radiation-dominated universe at last scattering, this relation is modified to become $\tau = aH_0^{-1}$. This is the reason for the shift to smaller angular scales, since a at last scattering is the same in both scenarios.

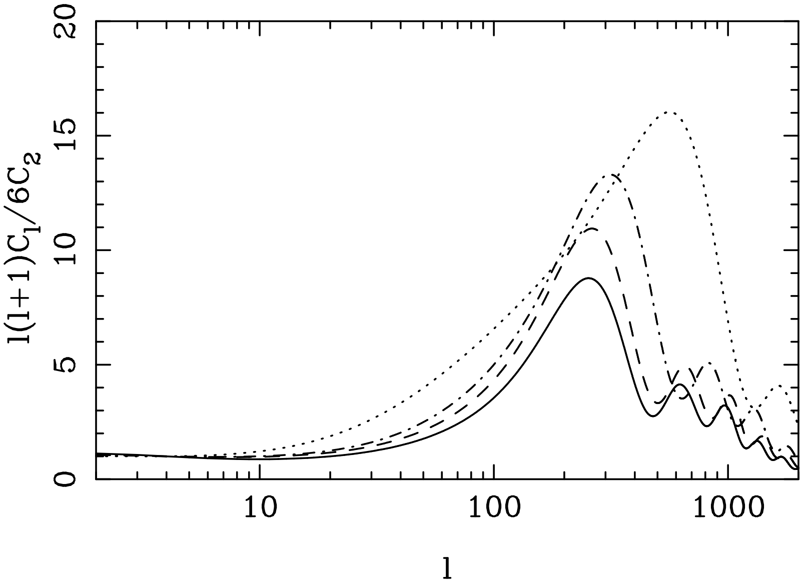

FIG. 5: CMB anisotropies for early-decaying models, corresponding to region-B of parameter space. The quadrupole-normalized anisotropy is plotted as a function of l. The solid line depicts ΛCDM. The dashed line represents a model with $\delta N_{rd} = 1.0$, the dashed-dotted has $\delta N_{rd} = 10.0$ and the dotted has $\delta N_{rd} = 100.0$. Each value of δN_{rd} corresponds to some α through Eq. 23, and thus to a one-parameter family of decaying neutrino models. Note that as δN_{rd} increase, the universe becomes less and less matter-dominated at recombination and the early-ISW peak becomes more prominent. For $\delta N_{rd} = 100$, the universe is very radiation-dominated at last scattering. This changes the age of the universe at recombination and shifts features to smaller values of l.

In the future, we will parameterize models in region-B in terms of the decay radiation density δN_ν. We should question the validity of this parameterization. We would expect that the complicating effect from massive neutrinos being present at last scattering is absent for $t_d \ll t_{ast}$, because in region-B the decaying neutrinos decay away when $t \sim t_d$. Furthermore, the collision terms in the Boltzmann equations for the decay radiation vanish for $t \gg t_d$, so that we expect that the decay radiation perturbations are well approximated by massless neutrinos. In this region we have the advantage that we can check this because we can calculate the CMB anisotropy properly. This is because region-B the neutrinos decay out-of-equilibrium, where our Boltzmann hierarchy for the decay radiation, Eq. 35, is valid. Because of this, it is possible to check the accuracy of this approximation. Specifically, we have checked that the calculated CMB spectrum in this region, for $t_d \ll t_{rec}$, is identical in the following two approaches: 1) adding a separate Boltzmann hierarchy, described by Eq. 35 for the decay radiation perturbations, and 2) simply increasing the effective number of massless neutrinos within a ΛCDM framework, using Eq. 23.

- C: $m_h > 3T(t_d)$, $t_{rec} < t_d < t_U$

In these models, the neutrinos decay out-of-equilibrium and after last scattering. The decay radiation is not present until after last scattering; the decays source anisotropy through the late-ISW effect. As for region-B, the amount of decay radiation at decay is determined by the parameter α. But for region-C, the parameter degeneracy is broken, because the scale of the late-ISW feature depends on the neutrino lifetime. The CMB spectra for several late-decaying models are shown in Figs 6, 7, 8. Note that the size of the ISW effect increases as m_h increases, for fixed t_d, and the location of the feature shifts to larger scales (smaller l) as t_d increases.

We can estimate the location of the late-ISW effect by noting that it is sensitive to the scale of the sound horizon

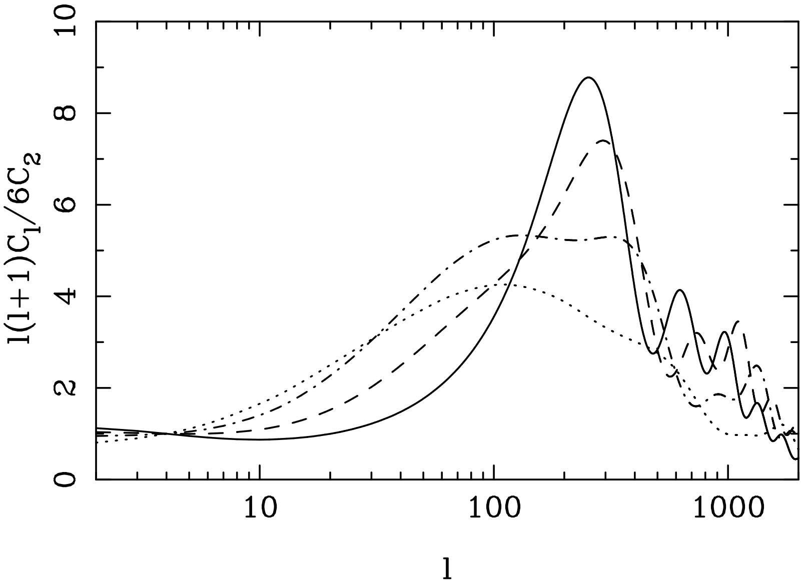

FIG. 6: CMB anisotropies for late-decaying models with $t_d = 10^{14}$ sec. The solid line represents the baseline ΛCDM model. The dashed line has $m_h = 10$ eV, the dashed-dotted line has $m_h = 31.4$ eV and the dotted has $m_h = 100$ eV. The decay radiation sources a late-ISW feature that becomes more prominent for larger masses.

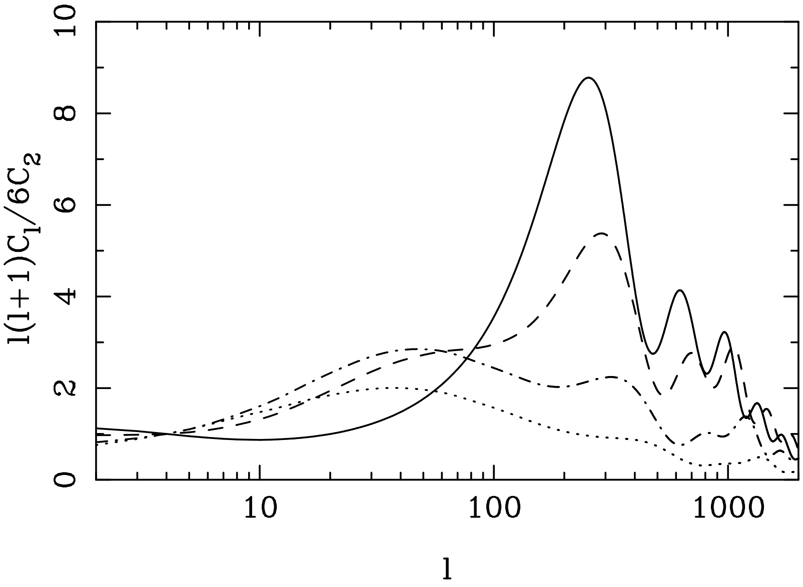

FIG. 7: CMB anisotropies for late-decaying models with $t_d = 10^{15}$ sec. The solid line represents the baseline ΛCDM model. The dashed line has $m_h = 10$ eV, the dashed-dotted line has $m_h = 31.4$ eV and the dotted has $m_h = 100$ eV. The late-ISW feature is shifted to larger angles relative to the $t_d = 10^{14}$ sec models.

at the time the potentials decay. For neutrinos that decay out-of-equilibrium, like those in regions-B and C, this time is near $t = t_d$, so that the location of the ISW induced feature is determined by the lifetime of the neutrino. For lifetimes shorter than the age of the universe, inhomogeneities on scales k project onto angular scales $\ell \sim k\tau_0$ where τ_0 is the conformal time today (we assume a flat universe). The potentials vary in time, and hence cause the ISW effect, most significantly at the time of decays on scales of order the sound horizon: $k_{sh}^2 \simeq 3/(4\tau_d^2 w)$ where $w = P/\rho$ is the averaged equation of state. Therefore, the bump in the spectrum is produced at $\ell \sim k_{sh}\tau_0 \simeq (\tau_0/\tau_d)(4w/3)^{-1/2}$. If the decay occurs after matter domination but before possible cosmological constant domination (which occurs only at very late times), then w is determined by the decay radiation. Since the epoch of matter-radiation equality is near recombination for the models we are considering, this assumption is valid for most of region-C. Hence $w \simeq \Omega_{rd}(t_d)/3$, where $\Omega_{rd}(t_d)$ is the fraction of critical

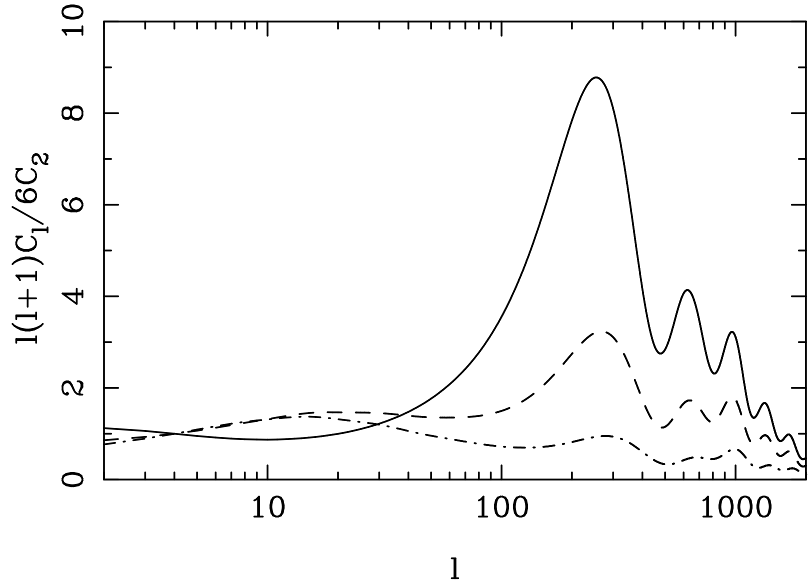

FIG. 8: CMB anisotropies for late-decaying models with $t_d = 10^{15}$ sec. The solid line represents the baseline ΛCDM model. The dashed line has $m_h = 10$ eV, the dashed-dotted line has $m_h = 31.4$ eV. The model with $m_h = 100$ eV is not shown since this model has $\Omega_{rd} > 1 - \Omega_B - \Omega_\Lambda = 0.22$, i.e., the model is in region-E. In these models, the late-ISW feature has significant power at the quadrupole, which suppresses the small angle anisotropy in this quadrupole-normalized plot. Of course, the normalization is allowed to vary in all subsequent analysis.

density in decay radiation at decay. If we assume that the decay radiation never dominates the universe, then we can estimate $\Omega_{rd}(t_d)$ in terms of the neutrino properties:

$$\Omega_{rd}(t_d) \simeq 1.7 \times 10^{-3} \, \frac{1}{h^2} \left(\frac{m_h}{\mathrm{eV}} \right)^{4/3} , \tag{46}$$

valid for $\Omega_{rd} \ll 1$. Since we are assuming that the universe is matter dominated at decay, physical times are related to conformal times by $\tau \propto t^{1/3}$. If, on the other hand, $\Omega_{rd}(t_d) \simeq 1$, then the decay radiation dominates until very late times, and we have the radiation-dominated expression $\tau \propto t^{1/2}$. We can combine these results to obtain an approximate expression for the location of the ISW peak for region-C:

$$l_{ISW} \simeq \begin{cases} 1200 \, h \, \alpha^{-1/3} & \text{if } m_h \ll 120 \, h^{3/2} \text{ eV} \\ 1.5 \sqrt{\frac{t_U}{t_d}} & \text{if } m_h \gtrsim 120 \, h^{3/2} \text{ eV} \end{cases} , \tag{47}$$

where $t_U \simeq 4 \times 10^{17}$ sec is the age of the universe. Entropy fluctuations, which occur when there are appreciable amounts of both matter and radiation, decrease the sound speed, thereby increasing l_{ISW}. The relative size of this effect is typically of order 20–40%.

- D: $t_d > t_U$

  In this region, the massive neutrino is effectively stable. Stable neutrinos have a long history as a dark matter candidate. Constraints on these models have been explored in Refs. [49, 51].

- E: $m_h < 3T(t_d)$, $m_h < 3T(t_{rec})$

  Here the neutrinos decay in equilibrium. Therefore, the energy density in radiation increases by $\delta N_\nu = 0.17$ after the neutrino becomes non-relativistic and decays away. However, since $m_h \lesssim 3T(\tau_*)$, this occurs after last scattering, with the exact time depending on m_h; the CMB anisotropy in this region are degenerate in τ_d. The small late-ISW effect that is induced is too small to be measured, even with future satellite-based experiments. For this reason, we will not study region-E any further.

- F: $m_h < T(t_d)$, $t_d > t_{rec}$

  Here, the density in either stable neutrinos or their decay radiation is enough to require $\Omega_0 > 1$. These models are extreme and suffer several problems, such as producing a universe that is too young, and so will not be analyzed further here.

VI. RESULTS

The goal of this section is to answer two questions. 1) Is the CMB anisotropy for some decaying neutrino model sufficiently different from baseline ΛCDM so that the two models are distinguishable? 2) Given a particular decaying neutrino model, how well can the cosmic parameters, including neutrino parameters, be measured? To answer question 1) we use the distinguishability framework of Sec. IV B and the Appendix, and to answer question 2) we use the Fisher matrix approach of Sec. IV A.

In both cases, we adopt the following ΛCDM model as our baseline: $\Omega_\Lambda = 0.7$, $\Omega_{CDM} = 0.22$, $\Omega_B = 0.08$, $h = 0.5$, Harrison-Zeldovich primordial spectrum ($n_s = 1.0$), reionization optical depth $\tau_* = 0.1$, and three massless species of neutrinos. The set of cosmic parameters allowed to vary was $\lambda_i = \{\Omega_\Lambda, \Omega_B, h, n_s, \tau_*, Q\}$, where Q is the overall normalization. To calculate the Fisher matrix α_{ij} we took two-sided derivatives for all of our cosmic parameters parameters as suggested in reference [11], i.e.,

$$\frac{\partial C_{Xl}}{\partial \lambda_i} = \frac{C_{Xl}(\lambda_i + \delta\lambda_i) - C_{Xl}(\lambda_i - \delta\lambda_i)}{2\delta\lambda_i}\,, \tag{48}$$

where $\delta\lambda_i$ is the numerical stepsize in the i-th cosmic parameter. All of our derivative stepsizes were taken to be 3% of their baseline values, except for τ_*, whose stepsize was 0.03. We verified numerically that the derivatives were stable with respect to varying the stepsizes. In calculating $\partial C_{Xl}/\partial\Omega_B$ and $\partial C_{Xl}/\partial\Omega_\Lambda$, we allowed Ω_{CDM} to vary, to maintain flat universe: $\Omega_{CDM} = 1 - \Omega_\Lambda - \Omega_B$. The baseline model and its derivatives are shown in Fig. 9.

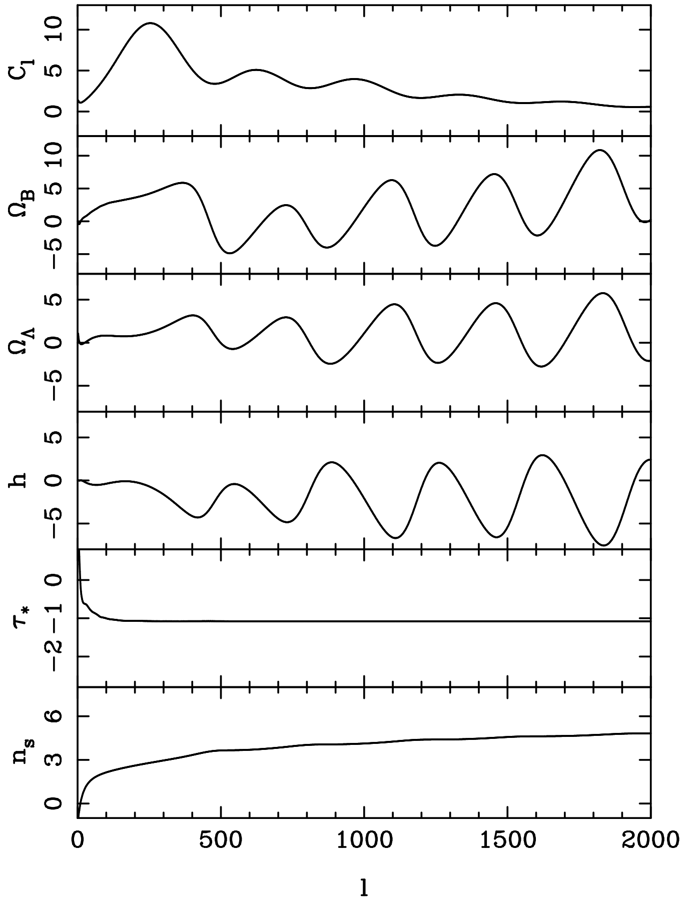

FIG. 9: Baseline ΛCDM model and its derivatives with respect to cosmic parameters. The top panel is the quadrupole-normalized baseline CMB spectrum: $\Omega_B = 0.08$, $\Omega_\Lambda = 0.7$, $h = 0.5$, $\tau_* = 0.1$, $n_s = 1.0$. The lower panels are derivatives with respect to Ω_B, Ω_Λ, h, n_s, and τ_*, normalized to the baseline spectrum: $1/C_{Xl}\ \partial C_{Xl}/\partial\lambda_i$. The derivative with respect to Q is not shown since $\partial C_{Xl}/\partial Q \propto C_{Xl}$.

From the CMB spectrum and its derivatives, we calculated the Fisher matrix, using Eq. 43. To analyze a real experiment requires understanding details like their window functions and experimental noise. However, for future satellite-based experiments like MAP and Planck, the experimental uncertainty is expected to be below cosmic variance

Parameter	$l_{max} = 1000$	$l_{max} = 2500$	$l_{max} = 1000$ (w/ pol.)	$l_{max} = 2500$ (w/ pol.)
Ω_B	5.16 %	2.01 %	2.27 %	0.700 %
Ω_Λ	4.02 %	1.26 %	1.71 %	0.391 %
h	3.56 %	1.05 %	1.46 %	0.323 %
n_s	1.46 %	0.340 %	0.665 %	0.194 %
τ	0.0803	0.0523	0.0579	0.0507
Q	5.75 %	5.29 %	5.37 %	5.24 %

TABLE I: Statistical uncertainties on cosmic parameters for the fiducial ΛCDM model for $l_{max} = 1000$ and for $l_{max} = 2500$, with and without polarization information. In all cases all cosmic parameters were allowed to vary simultaneously.

for most of the angular scales they are designed to measure, and the window functions are relatively narrow. This allows us to characterize the experiments as cosmic variance limited to some l_{max}, with the value of l_{max} determined by the experiment. We take $l_{max} = 1000$ for MAP and $l_{max} = 2500$ for Planck. For both values of l_{max} we consider cases with and without polarization information. The reason for this is that it is not certain how good polarization information will be. For the case that includes polarization, we assume cosmic-variance limited polarization information from a minimum $l_{min} = 200$ up to the same l_{max} as for the temperature data. The reason for the minimum value of l is that the large-scale polarization signal is small enough to be overwhelmed by the experimental noise of MAP and Planck. Our results are insensitive to the precise value of l_{min}. The statistical uncertainties on the cosmic parameters are shown for MAP and Planck in Tab. VI. In this work, we take the conservative (and realistic) approach of always marginalizing over all cosmic parameters simultaneously. In this case, Eq. 44 gives the statistical uncertainty on the parameters.

A. Ruling out models

We analyzed a grid of models, consisting of 20 masses with $\log(m_h/\mathrm{eV})$ evenly spaced from -1.0 to 1.40, and 13 lifetimes with $\log(t_d/\mathrm{sec})$ evenly spaced from 10.0 to 18.0. For each grid point, we followed the procedure given in Sec. IV B and the Appendix. An example of this procedure, for a late-decaying scenario, is shown in Fig. 10. There we show the ΛCDM and decaying neutrino spectrum, along with the best-fit perturbed ΛCDM model and the discrepancy in the fit in units of cosmic variance. From this discrepancy we calculate a confidence level for the model. The results for MAP and Planck are shown in Figs. 11 and 12. For MAP, stable neutrinos of masses greater than a couple of eV are distinguishable from the baseline model, while for Planck, the sensitivity extends down to masses of several tenths of an eV. As the lifetime decreases and the neutrino becomes unstable, but late-decaying, the sensitivity in mass decreases somewhat. This is because the late-ISW signature of a late-decaying neutrino is mostly degenerate with reionization. When the lifetime is short enough so that the neutrinos are decaying before last scattering, models with the same value of α are degenerate, and are distinguished at the same level. This is clear from a visual inspection of the plot. Finally, even the most optimistic case of Planck with polarization will not be able to distinguish equilibrium decaying models from ΛCDM.

For early-decaying neutrinos, we can obtain a clearer picture by exploiting the parameter degeneracy, describing the models with the single variable α. Fig. 13 shows the confidence level for models as a function of α. MAP will be able to distinguish models with $\alpha \gtrsim 10$ without polarization, and $\alpha \gtrsim 5$ with polarization. Planck, with or without polarization, will distinguish any out-of-equilibrium decaying models, with $\alpha \gtrsim 1$. This plot confirms the result that models in region-A, with $\delta N_\nu = 0.17$ at recombination, are indistinguishable from ΛCDM.

The formalism used to perform these distinguishability calculations is valid in a linear regime, where Eq. 51 holds. If the parameter biases become large then the formalism breaks down. Since some of the decaying neutrino models produce CMB anisotropy very different from the canonical ΛCDM, the linear approximation must break down for these models. However, the distinguishability contours can be believed if two facts hold. First, the linear approximation should hold for models that are just becoming indistinguishable, i.e., those along the contour lines in Figs. 11 and 12. Second, models that are inside the contour must stay indistinguishable. The first point we observe to be true numerically. The second point could break down in a couple of ways: a) the spectra start to look more like standard ΛCDM as we go inside a contour, or b) the spectra don't look like our baseline ΛCDM but instead look like some standard model with very perturbed parameters. Neither objection holds. The first is obviously false because for any fixed t_d, the decaying neutrino effects increase as we go inside the contour, increasing m_h. The second objection is only slightly more problematic. For late decaying neutrinos, the decaying neutrino feature is a late-ISW bump at some large angular scale - it's pretty easy to see that this cannot be mimicked by ΛCDM with perturbed cosmic parameters. For

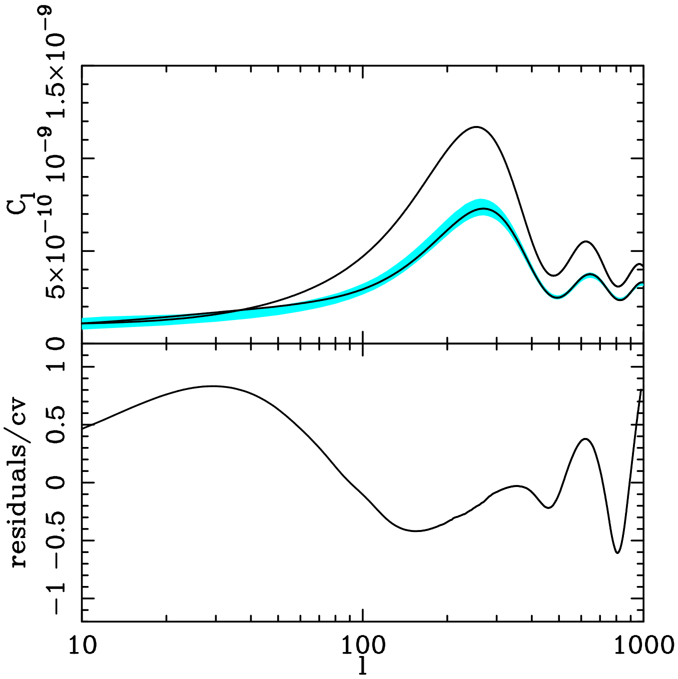

FIG. 10: Example of distinguishability analysis for a late-decaying neutrino scenario. Here $m_h = 3.23$ eV, and $t_d = 10^{16}$ sec. In the top panel the dashed line depicts the baseline ΛCDM model, with arbitrary normalization. The solid black line shows the decaying neutrino spectrum and the grey line shows the best-fit perturbed ΛCDM model. The thickness of the grey line represents cosmic variance. The bottom panel shows the difference between the decaying neutrino spectrum and the best-fit perturbed ΛCDM model, in units of cosmic variance. This model produces an ISW peak near $l = 25$, whose signature can clearly be seen in the bottom pane - no values of cosmic parameters in a ΛCDM model can reproduce such a feature. For MAP, without polarization, this model is ruled out at the 89.7 % level.

early decays, the early-ISW effect is degenerate with the ratio of matter density to radiation density at last scattering. But in this work the only non-standard physics we are allowing is the decaying neutrino itself. This allows us to fix this ratio for the set of ΛCDM models. Other cosmic parameters affect the relative amount of radiation at last scattering. In particular h, and Ω_Λ, are mostly degenerate with N_ν [33]. However, the degeneracy is not complete so that h and Ω_Λ cannot completely mimic the early-ISW signal for these models. Since we are considering models well within the distinguishability contours where the early-ISW signal is large, the lack of complete degeneracy prevents h and Ω_Λ from mimicking the decaying neutrino signal.

B. Measuring neutrino parameters

Here we are concerned with our ability to measure cosmic parameters, where the set includes quantities that specify the decaying neutrinos. We are primarily interested in the answers to two questions. First, what are the statistical uncertainties in the neutrino parameters? This goes to the goal of using the CMB as a probe of neutrino physics. Second, how much are the uncertainties in the non-neutrino cosmic parameters degraded by their presence? It is always true that adding extra parameters to the set increases or at best doesn't change the uncertainty in the existing parameters. If the extra parameters are orthogonal to the existing parameters in the sense that the change in the CMB spectrum from perturbing the new parameters cannot be mimicked by perturbing the existing parameters, then the degradation in the existing uncertainties is minimal. If, in the other extreme, the effect of perturbing new parameters can be mimicked by changing the existing parameters, the degradation is severe. Mathematically, this can be analyzed in terms of cross-correlations in the Fisher matrix: large cross-correlations mean degraded sensitivities. This degradation is one of the main arguments for pursuing the distinguishability calculations of the last section. If the CMB provides no evidence for decaying neutrinos, i.e., the real-universe CMB spectrum is not distinguishable from ΛCDM, then adding decaying neutrino parameters will be a hard sell.

Since the physics behind the CMB anisotropy is different for different regions of neutrino parameter space, there is no one best set of neutrino parameters to add to the cosmic parameters. We will group together the early-decaying neutrino models, corresponding to region-A and region-B, together, and use α as the sole neutrino parameter in this

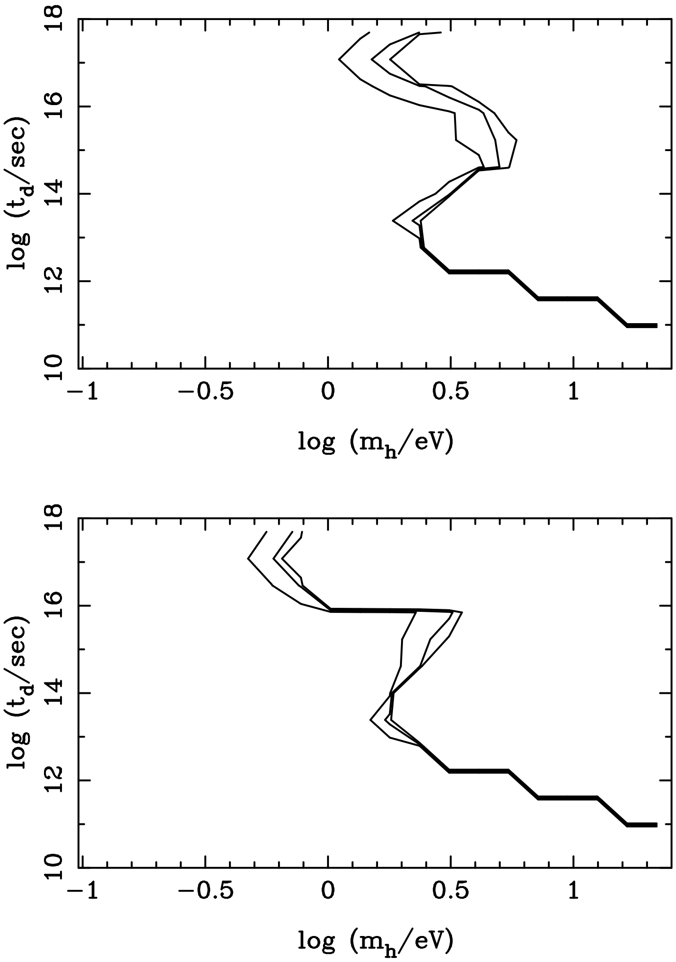

FIG. 11: Decaying neutrino parameter space, showing models that are distinguishable from ΛCDM. The three contours represent distinguishability at the 90%, 99.9% and 99.9% levels for the MAP experiment. In the top panel, temperature data is considered alone; the bottom panel includes polarization. Models to the right of the contours are distinguishable.

region. It is easier to compute the CMB spectra in terms of the radiation energy density N_ν, but α is more directly related to the mass and lifetime of the neutrino; the uncertainty in α can be related to the uncertainty in N_ν through the relation

$$\delta\alpha_{stat} = \delta N_{\nu,stat} \frac{\partial\alpha}{\partial N_\nu} \, , \tag{49}$$

where the derivative is obtained from a numerical solution to the Boltzmann equation, summarized in Fig. 3. For the late-decaying, but unstable neutrinos in region-C, we can just use the mass and lifetime as our neutrino parameters, (m_h, t_d). However, as the neutrinos become stable, in region-D, the inverse of the lifetime becomes a more natural parameter, since the baseline model corresponds to the limit $m_h \to 0$ and $1/t_d \to 0$. Therefore, we define an inverse-lifetime parameter, scaled to the lifetime of the universe,

$$y \equiv \frac{t_U}{t_d} \, , \tag{50}$$

and use the set (m_h, y) in region-D. Our parameter choices are summarized in Tab. II.

Fig. 14 shows the relative statistical uncertainty in α, versus α, for early-decaying models. Note that $\delta\alpha_{stat}/\alpha$ is a decreasing function of α. This is because the relative sensitivity to radiation energy density is roughly model-independent, i.e., $\delta N_{\nu,stat}/N_\nu$ is roughly constant. This means that $\delta\alpha_{stat}/\alpha \propto \alpha^{-2/3}$, for $\alpha \gg 1$. For $\alpha \ll 1$, the radiation density ceases to depend on α at all: $\delta\alpha_{stat}/\alpha \to \infty$ as $\alpha \to 0$. The value of α with $\delta\alpha_{stat} = \alpha$ is interesting because there ΛCDM, with $\alpha = 0$ is ruled out at the 1-σ level. For MAP, this point occurs at $\alpha \simeq 25$ without and $\alpha \simeq 5$ with polarization. For Planck, with or without polarization, this occurs near $\alpha = 1$. Models where the data

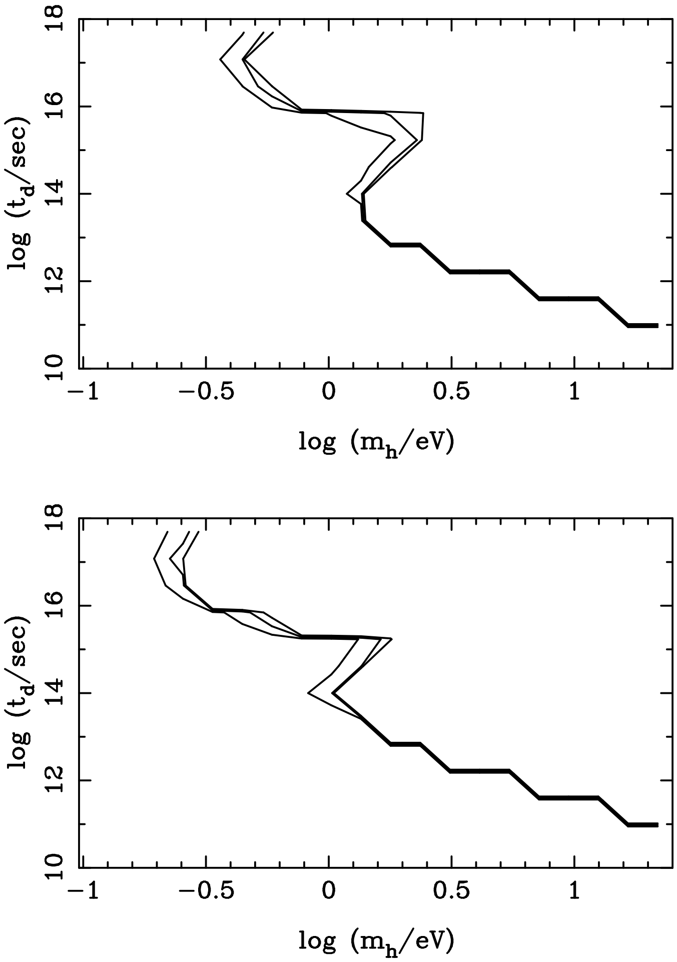

FIG. 12: Same as Fig. 11, but for the Planck experiment.

Region	Neutrino Parameter(s)
A	α (degenerate, with $\delta N_\nu = 0.17$)
B	α
C	$(m_h,\, t_d)$
D	$(m_h,\, y)$

TABLE II: Neutrino parameters to add to the set of cosmic parameters, for different regions of neutrino parameter space.

would rule out ΛCDM at high significance occur for only slightly higher values of α. These values should be compared to the distinguishability results from the last section, where distinguishable values of α were a factor of several higher. This represents the advantage of including neutrino parameters in the analysis: one can rule out more models this way.

This advantage comes at a price: the degradation in the ability to measure the non-neutrino parameters. First, consider $\alpha \lesssim 1$, where the decaying neutrino models produce CMB spectra very similar to ΛCDM,and the uncertainties in the cosmic parameters reflect the degradation that would occur if one added α (or δN_ν), and analyzed . The results for the limit $\alpha \to 0$ are shown in Tab VI B. Note that the *relative* degradation is much larger for MAP than for Planck, and that the degradation for certain parameters, Ω_B, h, n_s, is quite severe. Fig. 15, shows the statistical uncertainties in the other cosmic parameters as a function of α, also normalized to the uncertainties for ΛCDM. The table just discussed is the $\alpha \to 0$ limit of the figure. The most prominent feature of the figure is general trend towards lower sensitivity for increasing α.

The parameter uncertainties for several late-decaying models in region-C are shown in Tables VI B and VI B. The uncertainty in the neutrino parameters m_h and t_d increases as the lifetime increases from 10^{14} to 10^{16} sec. The reason

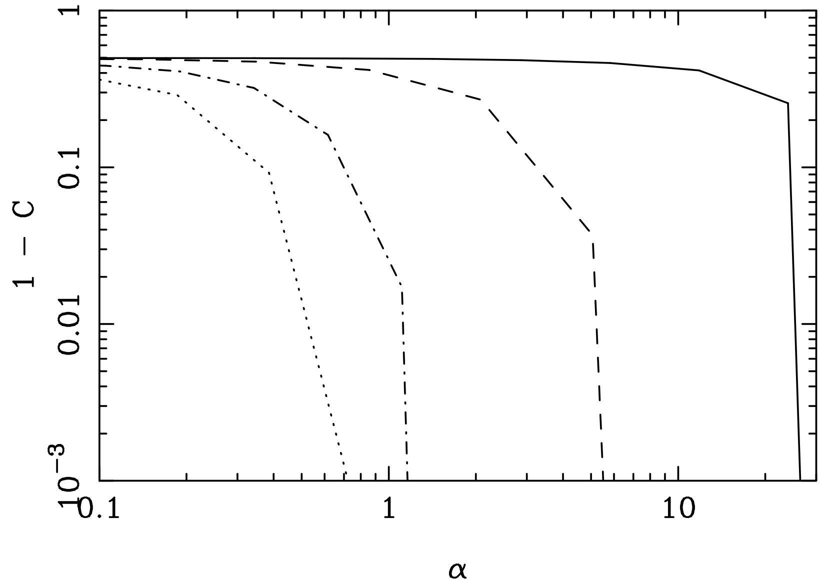

FIG. 13: Level at which early-decaying models are allowed, as a function of relativity parameter $\alpha = 0.087(m_h/\mathrm{MeV})^2(\mathrm{t_d}/\mathrm{sec})$, for $l_{max} = 1000$ without polarization (solid line), 1000 with polarization (dashed line), 2500 without polarization (dash-dotted line) and 2500 with polarization (dotted line). Equilibrium-decaying neutrinos, corresponding to region-A, have $\alpha < 1$, whereas neutrinos that decay out-of-equilibrium, region-B, have $\alpha > 1$. For two-body decays, $\delta N_\nu \to 0.17$ as $\alpha \to 0$. An experiment sensitive to $l_{max} = 2500$, with or without polarization information, will be sensitive to neutrinos on the border between equilibrium and out-of-equilibrium decay ($\alpha \sim 1$). Without polarization, an experiment sensitive only to $l_{max} = 1000$ can only probe very out-of-equilibrium decays ($\alpha > 100$); including polarization increases the sensitivity to $\alpha \simeq 5$. None of the cases considered will be able to distinguish equilibrium-decaying models from ΛCDM.

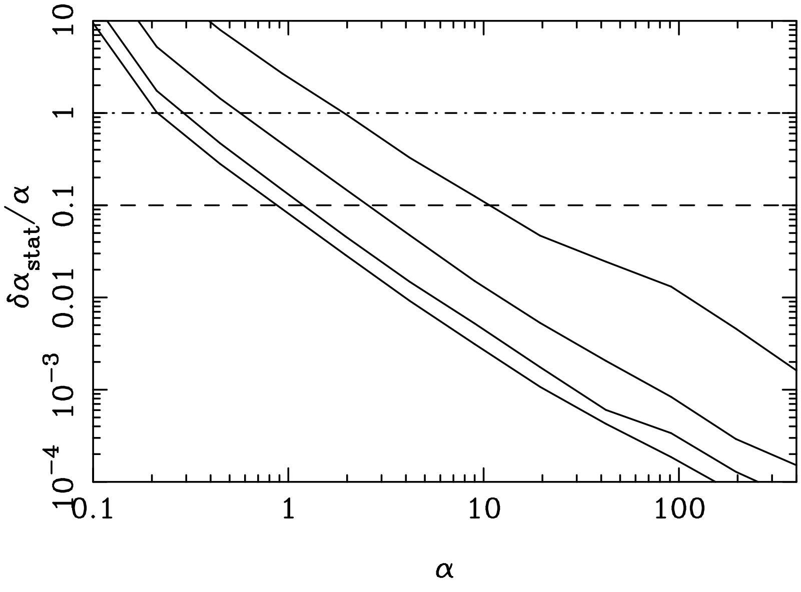

FIG. 14: Using the CMB to measure α for early-decaying neutrinos, corresponding to regions-A and B. The solid lines show the statistical uncertainty in the parameter α as a function of α. In order of increasing sensitivity, the solid lines correspond to $l_{max} = 1000$ (no polarization), $l_{max} = 1000$ (with polarization), $l_{max} = 2500$ (no polarization) and $l_{max} = 2500$ (with polarization). The dot-dashed line represents the case where the $\delta\alpha_{stat} = \alpha$; the dashed line shows $\delta\alpha_{stat} = 0.1\alpha$. For models below these lines, α can be measured to good relative accuracy.

for this is that the ISW peak for the lower lifetime neutrinos occurs at higher l, where two features work to improve the sensitivity. First, cosmic variance is lower. Second, a given range of angular scales translates to a larger number of l's. As for the other parameters, since we add two extra parameters to the analysis implies that we might expect relatively large uncertainties. This is observed for most parameters, especially for MAP. For some cases, the uncertainties are

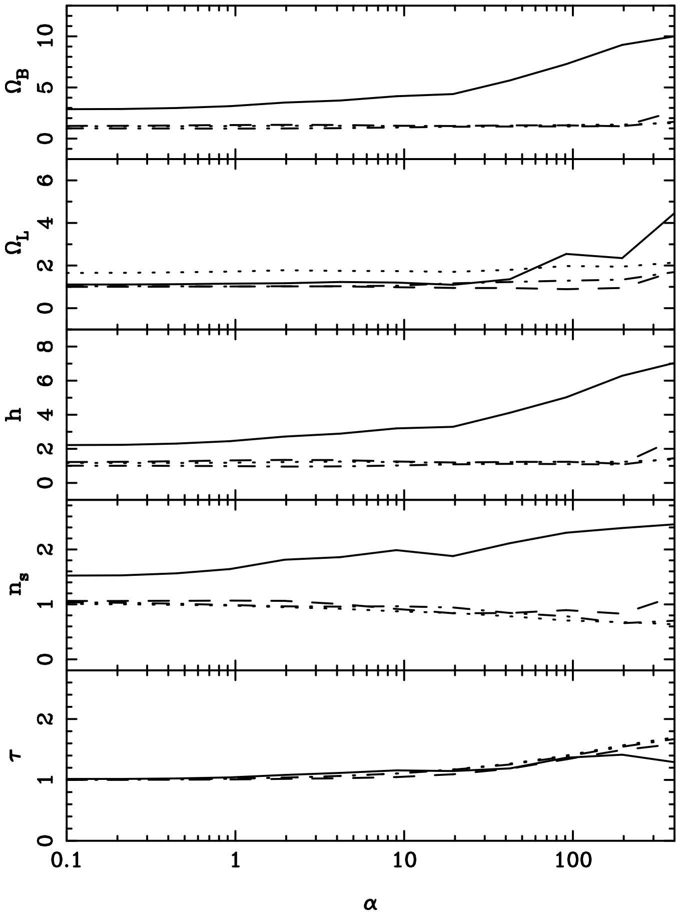

FIG. 15: Degradation in ability to measure the non-neutrino parameters, for early-decaying models. Each panel shows the statistical uncertainty in a cosmic parameter as a function of α. The uncertainties are normalized to the value obtained analyzing ΛCDM without decaying neutrino parameters. The different curves in each panel correspond to MAP without polarization (solid), MAP with polarization (long-dash), Planck without polarization (dash-dot), and Planck with polarization (dotted). As $\alpha \rightarrow 0$, the CMB anisotropy is close enough to ΛCDM so that in this limit the curves may be interpreted as the degradation caused by adding α as a parameter to ΛCDM.

Parameter	$l_{max} = 1000$	$l_{max} = 2500$	$l_{max} = 1000$ (polarization)	$l_{max} = 2500$ (polarization)
Ω_B	2.85	1.00	1.23	1.21
Ω_Λ	1.11	1.03	1.00	1.65
h	2.21	1.01	1.21	1.18
n_s	1.52	1.04	1.06	1.02
τ	1.02	1.00	1.00	1.00
Q	1.01	1.00	1.00	1.00

TABLE III: Statistical uncertainties in non-neutrino parameters for $\alpha = 0$, i.e., where α is added as a cosmic parameter. The results are shown normalized to the case where the data is analyzed without neutrino parameters. Therefore, the numbers represent the degradation in sensitivity from including non-neutrino parameters. Results are shown for $l_{max} = 1000$, and 2500, with and without polarization.

actually less than for ΛCDM, which appears to violate the requirement that adding cosmic parameters *decreases* the sensitivity in the other parameters. However, here it doesn't make sense to talk about degradation, since the CMB spectra for these models is very different from (these models are all distinguishable - see Figs. 11 and 12).

The results for several almost-stable scenarios are shown in Tables VI B and VI B. The relative degradations in the non-neutrino parameters become worse as y increases because there the CMB anisotropy starts to be affected by the decay products. For very low values of y, the uncertainty degradations are the same as the case for stable neutrinos,

Model	m_h	t_d	Ω_B	Ω_Λ	h	n_s	τ_*	Q
$m_h = 10$ eV, $t_d = 10^{14}$ sec	2.15	8.05	26.1	16.1	14.1	2.67	83.4	6.77
			(5.06)	(4.00)	(3.97)	(1.82)	(1.04)	(1.18)
	1.21	5.59	4.12	2.34	2.05	0.403	82.2	5.40
			(1.81)	(1.36)	(1.40)	(0.60)	(1.42)	(1.00)
$m_h = 10$ eV, $t_d = 10^{15}$ sec	2.46	13.1	33.2	22.1	18.6	3.44	49.6	7.79
			(6.44)	(5.51)	(5.22)	(2.35)	(0.62)	(1.35)
	1.12	11.8	4.83	3.08	2.53	0.436	45.4	7.51
			(2.13)	(1.80)	(1.73)	(0.656)	(0.784)	(1.40)
$m_h = 10$ eV, $t_d = 10^{16}$ sec	15.6	54.4	28.2	21.5	15.2	2.57	122.	7.20
			(4.46)	(5.34)	(4.27)	(1.75)	(1.52)	(1.25)
	11.4	44.9	9.46	8.96	4.68	0.827	90.7	6.69
			(4.17)	(5.23)	(3.20)	(1.24)	(1.57)	(1.25)
$m_h = 3.16$ eV, $t_d = 10^{14}$ sec	6.18	25.7	13.8	8.53	7.63	1.77	105.	6.98
			(2.68)	(2.12)	(2.14)	(1.21)	(1.31)	(1.21)
	3.14	15.3	5.04	2.82	2.53	0.654	90.2	6.53
			(2.22)	(1.65)	(1.73)	(0.983)	(1.56)	(1.21)
$m_h = 3.16$ eV, $t_d = 10^{15}$ sec	6.91	43.6	13.1	8.73	7.65	1.52	71.8	7.10
			(2.53)	(2.17)	(2.15)	(1.04)	(.894)	(1.23)
	4.02	36.7	4.90	2.98	2.56	0.537	70.1	6.62
			(2.16)	(1.74)	(1.76)	(0.807)	(1.21)	(1.23)
$m_h = 3.16$ eV, $t_d = 10^{16}$ sec	23.0	119.	18.3	10.9	10.1	1.74	146.	7.94
			(3.54)	(2.72)	(2.83)	(1.19)	(1.82)	(1.38)
	12.6	50.3	6.28	4.35	3.28	0.675	80.5	7.12
			(2.77)	(2.53)	(2.24)	(1.02)	(1.39)	(1.33)

TABLE IV: Using the MAP experiment to measure m_h and t_d for late-decaying neutrinos. The statistical uncertainties on the cosmic parameters, $\delta\lambda_i/\lambda_i$, in percent, are shown for several models. The number in parenthesis is the ratio of the uncertainty to the uncertainty for ΛCDM. For each model the top row of data is for temperature data only and the bottom row includes polarization.

with m_h as the sole additional cosmic parameter. A prominent feature of the data here is that for both MAP and Planck, $\delta y \gg y$ for $y \ll 1$; it is impossible to use the CMB to probe neutrino decays in the almost-stable limit. This is because the late-ISW feature is imprinted at very low values of l where the cosmic variance is high and where there are few l's to measure.

VII. SUMMARY

The goal of this work was a study of using anisotropy in the CMB to constrain the physics of neutrinos that decay into non-interacting daughter products. We presented the formalism required to compute the CMB anisotropy spectra in these models. This required calculating the energy densities and the perturbations in the decaying neutrino and its decay products, and incorporating this physics into the CMBFAST code [47]. We divided the decaying neutrino parameter space into regions, delineated by significant physical scales, and discussed the physics behind the CMB spectra in each region. An enhanced early or late integrated-ISW effect is the main effect for most of the neutrino parameter space.

We then developed analytic methods, valid in the linear regime, to determine when a model is distinguishable from

Model	m_h	t_d	Ω_B	Ω_Λ	h	n_s	τ_*	Q
$m_h = 10$ eV, $t_d = 10^{14}$ sec	0.94	4.89	2.18 (1.08)	1.14 (0.913)	1.02 (0.972)	0.345 (1.01)	81.1 (1.55)	5.45 (1.03)
	0.453	3.42	0.539 (0.770)	0.349 (0.891)	0.273 (0.844)	0.190 (0.978)	80.4 (1.58)	5.35 (1.02)
$m_h = 10$ eV, $t_d = 10^{15}$ sec	1.12	10.1	2.25 (1.12)	1.40 (1.12)	1.11 (1.05)	0.242 (0.712)	45.6 (0.873)	7.55 (1.43)
	0.825	8.17	0.727 (1.04)	0.739 (1.89)	0.400 (1.24)	0.173 (0.889)	43.8 (0.863)	6.74 (1.29)
$m_h = 10$ eV, $t_d = 10^{16}$ sec	3.25	13.2	2.88 (1.43)	2.05 (1.64)	1.50 (1.42)	0.363 (1.07)	28.4 (0.544)	3.90 (0.737)
	2.07	8.27	0.973 (1.39)	1.22 (3.11)	0.483 (1.49)	0.237 (1.21)	21.4 (0.421)	3.62 (0.691)
$m_h = 3.16$ eV, $t_d = 10^{14}$ sec	2.23	16.6	2.08 (1.03)	1.14 (0.910)	0.997 (0.945)	0.570 (1.68)	84.2 (1.61)	6.14 (1.16)
	1.21	12.0	0.634 (0.906)	0.355 (0.907)	0.280 (0.866)	0.338 (1.74)	73.59 (1.45)	5.89 (1.12)
$m_h = 3.16$ eV, $t_d = 10^{15}$ sec	3.24	28.6	2.10 (1.05)	1.28 (1.02)	1.09 (1.03)	0.407 (1.20)	67.5 (1.29)	6.25 (1.18)
	2.48	20.7	0.726 (1.04)	0.666 (1.70)	0.362 (1.12)	0.273 (1.41)	66.6 (1.31)	5.78 (1.10)
$m_h = 3.16$ eV, $t_d = 10^{16}$ sec	5.35	18.9	2.62 (1.31)	1.50 (1.19)	1.35 (1.28)	0.524 (1.54)	46.6 (0.891)	6.65 (1.26)
	3.36	9.63	0.876 (1.25)	0.749 (1.91)	0.434 (1.34)	0.318 (1.63)	36.1 (0.712)	6.40 (1.22)

TABLE V: Same as last table, but for Planck.

some canonical model like ΛCDM. With temperature data alone MAP can distinguish stable neutrino models from ΛCDM if the neutrino mass $m_h \gtrsim 2$ eV. Adding polarization data, $m_h \gtrsim 0.5$ eV is distinguishable. Planck can distinguish $m_h \gtrsim 0.5$ eV with temperature alone, and $m_h > 0.25$ eV with polarization. MAP without polarization can distinguish out-of-equilibrium, early-decaying models as long as $(m_h/\mathrm{MeV})^2\,\mathrm{t_d}/\mathrm{sec} \gtrsim 230$, and with polarization if $(m_h/\mathrm{MeV})^2\,\mathrm{t_d}/\mathrm{sec} \gtrsim 150$. For Planck without polarization, models with $(m_h/\mathrm{MeV})^2\,\mathrm{t_d}/\mathrm{sec} \gtrsim 9$ are distinguishable, and with polarization if $(m_h/\mathrm{MeV})^2\,\mathrm{t_d}/\mathrm{sec} \gtrsim 6$. Models in which neutrinos decay in equilibrium are indistinguishable from ΛCDM. Late-decaying models ($10^{13}\mathrm{sec} \lesssim \mathrm{t_d} \lesssim 4 \times 10^{17}\mathrm{sec}$) are distinguishable from ΛCDM if $m_h \gtrsim 5$ eV for MAP and $m_h \gtrsim 2$ eV for Planck.

Next, we studied the use of future CMB satellite data to measure cosmic parameters, including neutrino properties. The sensitivity to neutrino parameters depends strongly on the parameters themselves. We found that including neutrino parameters in a model significantly degrades the sensitivity to Ω_B, h, and n_s, and that the degradation is worse for MAP than Planck. For models whose CMB spectra are not close to ΛCDM, the situation is less simple, but the sensitivities to cosmic parameters are usually less than for the canonical case. For early-decaying models, the sensitivities to most non-neutrino parameters decreases as α increases. In addition, we calculated the set of models (for early-decaying neutrinos, for now), where the statistical uncertainty in the neutrino parameters is low enough relative to the parameters themselves, to count as a detection of decaying neutrinos. For early-decaying neutrinos, MAP with can achieve this if $\alpha \gtrsim 10$ with temperature information alone, and if $\alpha \gtrsim 3$ with polarization data. The equivalent sensitivities for Planck are for $\alpha \gtrsim 1$ with temperature information alone, and $\alpha \gtrsim 0.8$ with polarization data

Model	m_h	y	Ω_B	Ω_Λ	h	n_s	τ_*	Q
$m_h = 1.0$ eV, $y = 0.1$	23.9	1050.	9.29 (1.81)	7.79 (1.94)	5.00 (1.41)	1.60 (1.09)	113. (1.42)	7.23 (1.26)
	12.7	898.	5.11 (2.25)	5.34 (3.12)	2.66 (1.82)	0.731 (1.10)	88.9 (1.54)	6.81 (1.27)
$m_h = 1.0$ eV, $y = 1.0$	25.5	349.3	14.9 (2.89)	11.6 (2.90)	7.43 (2.09)	1.72 (1.17)	149. (1.86)	7.29 (1.27)
	13.4	203.	6.20 (2.74)	5.45 (3.18)	3.08 (2.11)	0.903 (1.36)	95.9 (1.66)	6.39 (1.19)
$m_h = 3.16$ eV, $y = 0.1$	148.	394.	18.9 (3.67)	6.68 (1.66)	5.90 (1.66)	3.83 (2.60)	249. (3.12)	7.59 (1.32)
	15.5	331.	4.61 (2.03)	5.69 (3.32)	2.46 (1.68)	0.837 (1.26)	99.2 (1.71)	7.47 (1.39)
$m_h = 3.16$ eV, $y = 1.0$	210.	252.	31.5 (6.10)	11.0 (2.75)	11.3 (3.17)	5.73 (3.91)	316. (3.94)	6.81 (1.18)
	17.1	67.5	6.40 (2.82)	6.20 (3.62)	3.27 (2.23)	1.09 (1.63)	110. (1.91)	6.09 (1.14)

TABLE VI: Using the CMB to measure m_h and y for nearly stable neutrinos, for MAP. The statistical uncertainties on the cosmic parameters, $\delta\lambda_i/\lambda_i$, in percent, are shown for several models. The number in parenthesis is the ratio of the uncertainty to the uncertainty for ΛCDM. For each model the top row of data is for temperature data only; the bottom row includes polarization.

Model	m_h	y	Ω_B	Ω_Λ	h	n_s	τ_*	Q
$m_h = 1.0$ eV, $y = 0.1$	8.16	291.	2.88 (1.43)	2.17 (1.72)	1.44 (1.37)	0.410 (1.20)	57.1 (1.09)	5.47 (1.03)
	4.23	152.	0.950 (1.36)	0.909 (2.32)	0.465 (1.44)	0.227 (1.17)	52.5 (1.04)	5.25 (1.02)
$m_h = 1.0$ eV, $y = 1.0$	10.5	128.	3.51 (1.75)	3.21 (2.56)	1.82 (1.72)	0.540 (1.59)	69.7 (1.33)	5.79 (1.09)
	5.05	56.4	1.15 (1.64)	1.24 (3.16)	0.575 (1.78)	0.289 (1.49)	51.9 (1.02)	5.39 (1.03)
$m_h = 3.16$ eV, $y = 0.1$	4.64	159.	3.22 (1.60)	3.15 (2.51)	1.69 (1.60)	0.550 (1.62)	66.4 (1.27)	5.73 (1.08)
	2.94	62.8	1.12 (1.60)	1.19 (3.04)	0.576 (1.78)	0.228 (1.17)	49.6 (0.978)	5.27 (1.01)
$m_h = 3.16$ eV, $y = 1.0$	5.74	51.0	4.60 (2.29)	4.37 (3.48)	2.38 (2.25)	0.686 (2.02)	83.7 (1.60)	5.46 (1.03)
	3.67	20.6	1.40 (2.01)	1.50 (3.82)	0.727 (2.25)	0.389 (2.00)	51.5 (1.01)	5.03 (0.959)

TABLE VII: Same as Tab. VI B, but for Planck.

Although presented in the context of decaying neutrino cosmologies, the techniques developed here could easily be extended to more generic scenarios involving decaying particles which decay into sterile daughter products. The main difference in the calculation would be in determining the particle's initial abundance (the relativistic decoupling of the decaying neutrino simplifies the calculation in this case). Given this, the equations for the evolution of the densities and perturbations would be the same as for decaying neutrinos.

In conclusion, future CMB observations promise to provide a powerful probe of neutrino physics, over a wide range of parameter space not easily accessed by other means. A couple of caveats are in order. First, this investigation was preliminary in nature. Cosmic variance limited data is a best case scenario; real-world issues like foreground subtraction will complicate the actual data analysis. Hopefully, the data from MAP and Planck will approach this ideal. Second, the real world CMB anisotropy might look nothing like any variant of CDM, with or without decaying neutrinos. In this case, of course, the analysis presented here would no longer be valid; one would first have to understand the background cosmology before going on to study the impact of decaying neutrinos.

Acknowledgments

Thanks to Michael Turner for reviewing this paper and providing many helpful comments. Thanks to Scott Dodelson, Robert Scherrer, Manoj Kaplinghat and Lloyd Knox for helpful discussions. Thanks to Uros Seljak and Matthias Zaldarriaga for the use of the CMBFAST code. This work was supported through the DOE at Chicago and Fermilab and by NASA grant NAG 5-7092 (at Fermilab).

DISTINGUISHABILITY OF MODELS

This appendix deals with the question of how to determine whether or not the CMB spectra from massive decaying neutrino models are distinguishable from some baseline model like ΛCDM, which does not contain decaying neutrinos. Here we will restrict ourselves to the case where the decaying neutrino model produces CMB spectra that are only slightly different from the baseline.

We consider the following scenario. The universe actually contains decaying neutrinos, but the experimental data is analyzed without considering this possibility: the set of cosmic parameters does not include m_h or t_d. As a result, two things can happen. One, the cosmic parameters measured will in general be unequal to the true cosmic parameters, i.e., the results will be biased. Two, the best-fit spectra may be a poor fit. If, for example, the presence of the decaying neutrinos changed the spectrum in exactly the same way as adding a little extra baryon density, then the measured baryon density would be biased, but the best fit model would fit very well. It would be impossible to disentangle the decaying neutrino signature from the data. We will call a model *distinguishable* if the best fit model is a poor one.

To be more quantitative, we need to work through how one measures the cosmic parameters from the data. Start with some definitions: let $\{\lambda_i\}$ be the set of cosmic parameters considered. Here, $i = 1 \ldots N$, with N the total number cosmic parameters. As mentioned, this set does not include m_h or t_d. Let $\{\tilde{\lambda}_i\}$ be the set of true cosmic parameters, and $\{\lambda'_i\}$ be measured cosmic parameters. Finally, let $\{\delta\lambda_i\}$ be the parameter biases induced by the decaying neutrino's, i.e., $\lambda'_i \equiv \tilde{\lambda}_i + \delta\lambda_i$. The measured cosmic parameters are determined by minimizing a χ^2 statistic that is a function of $\{\lambda_i\}$, given by Eqn. 38. Here we will assume that the experimental uncertainties are just cosmic variance up to some maximum value of $l = l_{max}$, so that the covariance matrix is that given in Eqns. 39 and 40.

We know that the solution for the measured cosmic parameters with no decaying neutrinos and no noise is $\{\lambda_i\} = \{\tilde{\lambda}_i\}$. Now assume that the parameter biases, $\delta\lambda_i$, are small enough so that the following holds:

$$C_{Xl}^{theory}(\{\lambda'_i\}) \simeq C_{Xl}^{theory}(\{\tilde{\lambda}_i\}) + \frac{\partial C_{Xl}^{theory}}{\partial \lambda_k}\delta\lambda_k\,. \tag{51}$$

If the experiment measures the temperature anisotropy only, then $X = T$. With polarization information, $X = T, P, C$. This equation quantifies the statement that the anisotropy is only slightly different than for ΛCDM. If this holds we can solve for the parameter biases:

$$\delta\lambda_k = (\alpha_{jk})^{-1} \sum_l \sum_{XY} \frac{\partial C_{Xl}^{theory}}{\partial \lambda_j} V_{XYl}^{-1} S_{Yl}\,, \tag{52}$$

where S_{Xl} is the "signal":

$$S_{Xl} = C_{Xl}^{data} - C_{Xl}^{theory}\,, \tag{53}$$

and α_{jk} is the Fisher matrix, given in Eqn. 43. Finally, the best-fit χ^2 is given by

$$\chi^2_{min} = \sum_l \sum_{XY} \left(S_{Xl} - \delta\lambda_j \frac{\partial C^{theory}_{Xl}}{\partial \lambda_j} \right) V^{-1}_{XYl} \left(S_{Yl} - \delta\lambda_j \frac{\partial C^{theory}_{Yl}}{\partial \lambda_j} \right) \tag{54}$$

To determine whether or not a model is distinguishable, we will need to understand the statistical properties of $\left\langle \chi^2_{min} \right\rangle$, considered as an ensemble over different realizations of cosmic variance "noise"[57]. To develop the formalism for estimating the contributions to χ^2_{min} from noise and signal, we break the data spectrum C^{data}_l into two components:

$$C^{data}_{Xl} = C^{data,0}_{Xl} + N_{Xl}\,, \tag{55}$$

where $C^{data,0}_{Xl}$ is the decaying neutrino spectrum without noise, and N_{Xl} is the noise. In a perfect experiment, N_{Xl} is cosmic variance. The signal S_{Xl} breaks up similarly: $S_{Xl} = S^0_{Xl} + N_{Xl}$. Then the best-fit χ^2 can be written

$$\chi^2_{min} = \sum_l \sum_{XY} \left(S_{Xl} - \delta\lambda_j \frac{\partial C^{theory}_{Xl}}{\partial \lambda_j} + N_{Xl} \right) V^{-1}_{XYl} \left(S_{Yl} - \delta\lambda_j \frac{\partial C^{theory}_{Yl}}{\partial \lambda_j} + N_{Yl} \right)\,, \tag{56}$$

where $\delta\lambda_j$ is the CP bias for *noiseless* data, i.e., without cosmic variance.

Consider an ensemble of experiments for a given decaying neutrino model. Each experiment will have the same noiseless signal, but the noise, a random variable, will be different each time. Therefore, the value of χ^2_{min} will also vary. Associated with each value of χ^2_{min} is some probability that the ΛCDM model is allowed, denoted a. This probability is just the 1 minus the cumulative distribution function, $\mathcal{E}$, for the χ^2 distribution with $l_{max} - 1$ degrees of freedom, evaluated at χ^2_{min}:

$$a(\chi^2_{min}) = 1 - \mathcal{E}(l_{max} - 1, \chi^2_{min})\,. \tag{57}$$

Then the confidence level for ΛCDM, denoted $\mathcal{C}$, can be expressed as a convolution of a with the probability $P(\chi^2_{min})$ of obtaining different values of χ^2_{min},

$$\mathcal{C} = 1 - \int_0^\infty d\chi^2_{min} P(\chi^2_{min}) \left[1 - \mathcal{E}(l_{max} - 1, \chi^2_{min}) \right]\,. \tag{58}$$

To proceed further, we need to understand the shape of $P(\chi^2_{min})$, which is determined by the distribution of N_l.

We will treat the N_l's as Gaussian random variables with zero mean and variance determined by cosmic variance. In this limit $P(\chi^2_{min})$ is Gaussian too. However, the N_l's are not really Gaussianly distributed. A more realistic treatment [54] reveals that their distribution is closer to log-normal, with large high-N_l tails. The disagreement is greater for low values of l; for high values, say with $l \gtrsim 50$, the distribution is approximately normal. There are a couple of reasons why it is acceptable to approximate their distributions as normal. First, most of the statistical weight in distinguishing models comes from high values of l, because cosmic variance is smaller there and for experiments we will be considering, with $l_{max} \sim 1000$, there are just more values of l that are large than small. Second, many different distributions, one for each N_l, collectively determine the statistical properties of the χ^2_{min} distribution, and as the number of contributions becomes large, $P(\chi^2_{min})$ will tend towards a Gaussian. In this case $P(\chi^2_{min})$ is specified completely by its mean (or expectation value) $\left\langle \chi^2_{min} \right\rangle$, and its and variance

$$\sigma^2_\chi = \left\langle \left(\chi^2_{min} \right)^2 \right\rangle - \left\langle \chi^2_{min} \right\rangle^2\,. \tag{59}$$

First, the mean. Expanding the quadratic in Eqn. 56, we will have terms proportional to N_{Xl} and $N_{Xl}N_{Yl}$ and terms independent of N_{Xl}. The expectation of the linear term is zero, since $\langle N_{Xl} \rangle = 0$, as N_{Xl} is a Gaussian random variable with mean 0. For the quadratic term, $\langle N_{Xl} N_{Yl} \rangle = 2C^2_{Xl}/(2l+1)\delta_{XY}$, where δ_{XY} is the discrete delta function. Therefore, we find for the expectation value of χ^2_{min},

$$\left\langle \chi^2_{min} \right\rangle = \sum_l \sum_{XY} \left(S^0_{Xl} - \delta\lambda_j \frac{\partial C^{theory}_{Xl}}{\partial \lambda_j} \right) V^{-1}_{XYl} \left(S^0_{Yl} - \delta\lambda_j \frac{\partial C^{theory}_{Yl}}{\partial \lambda_j} \right) + \sum_l \sum_X V^{-1}_{XX} \frac{2C^{theory}_{Xl}}{2l+1}\,. \tag{60}$$

This expression simplifies in certain cases. Namely, if temperature and polarization data can be considered uncorrelated then $X = T, P$ and V^{-1}_{XY} is a diagonal matrix, with $V^{-1}_{XX} = (2l+1)/2C^2_{Xl}$. Then the second term on the right hand side of the last equation is just equal to the number of terms in the sum, $2(l_{max}-1)$, and the expectation value becomes

$$\left\langle \chi^2_{min} \right\rangle = 2(l_{max}-1) + \sum_l \sum_{X=T,P} \frac{2(l+1)}{2C^2_{Xl}} \left(\frac{\partial C^{theory}_{Yl}}{\partial \lambda_j} - S^0_{Xl} \right)^2 \tag{61}$$

The variance is an unholy mess. The second term on the right hand side is the square of the mean. The first term looks like the following:

$$\left\langle \left(\chi^2_{min}\right)^2 \right\rangle = \left\langle \sum_{lm} \sum_{WXYZ} \left(N_{Xl} + D_{Xl}\right) V^{-1}_{XYl} \left(N_{Yl} + D_{Yl}\right) \left(N_{Wm} + D_{Wm}\right) V^{-1}_{WZm} \left(N_{Zm} + D_{Zm}\right) \right\rangle \tag{62}$$

where

$$D_{Xl} = S^0_{Xl} - \delta\lambda_j \frac{\partial C^{theory}_{Xl}}{\partial \lambda_j} \tag{63}$$

doesn't depend on N_{Xl}.

If the temperature and polarization are uncorrelated, this equation simplifies considerably. The sum inside the brackets will contain different powers of N_{Xl} and N_{Xm}, the objects whose expectation values are non-trivial. Note that if the power of either N_l or N_m is odd, then that term's expectation value will vanish. In addition, terms that involve only N_l^2 or N_m^2 have already been discussed. This allows the expression to be greatly simplified:

$$\begin{aligned} \left\langle \left(\chi^2_{min}\right)^2 \right\rangle \; = \; & \left(\sum_l \sum_{X=T,P} \frac{2l+1}{2C^2_{Xl}} D^2_{lM} \right)^2 + 4\left(l_{max}-1\right) \left(\sum_l \sum_{X=T,P} \frac{2l+1}{2C^2_{Xl}} D^2_{lM} \right) + \\ & \sum_{l,m} \sum_{X,Y=T,P} \frac{2l+1}{2C^2_{Xl}} \frac{2m+1}{2C^2_{Yl}} \left\langle N^2_l \, N^2_m \right\rangle . \end{aligned} \tag{64}$$

The last term on the right hand side can be evaluated by noting the following identities: $\left\langle N^2_{Xl} N^2_{Xl} \right\rangle = 3(2C^2_{Xl}/(2l+1))^2$, and $\left\langle N^2_{Xl} N^2_{Ym} \right\rangle = (2C^2_{Xl}/(2l+1))(2C^2_{Ym}/(2l+1))$ if $X \neq Y$ or $l \neq m$. Using these identities, we find a simple formula for the variance:

$$\sigma^2_\chi = 4\left(l_{max}-1\right) . \tag{65}$$

Note that the formula depends only on the number of degrees of freedom and not on $\left\langle \chi^2_{min} \right\rangle$. Finally, we can express Eqn. 58 in terms of the probability distribution for χ^2_{min},

$$\mathcal{C} = 1 - \int_0^\infty d\chi^2 \frac{1 - \mathcal{E}(l_{max}-1, \chi^2)}{\sqrt{2\pi}\,\sigma_\chi} \exp\left[\frac{-\left(\chi^2 - \left\langle \chi^2 \right\rangle\right)^2}{2\sigma^2_\chi} \right] . \tag{66}$$

---

[1] J. R. Bond and M. White, Astrophys. J. **480**, 6 (1997).
[2] P. de Bernardis *et al.*, Astrophys. J. **480**, 1 (1997).
[3] C. H. Lineweaver, Astrophys. J. **505**, L69 (1998).
[4] S. Hancock *et al.*, Mon. Not. Roy. Ast. Soc. **294**, 1 (1998).
[5] J. Lesgourgues *et al.*, astro-ph/9807019 (1998).
[6] J. Bartlett *et al.*, astro-ph/9804158 (1998).
[7] J. R. Bond and A. H. Jaffee, astro-ph/9808043 (1998).
[8] A. M. Webster, Astrophys. J. **509**, L65 (1998).
[9] M. White, Astrophys. J. **506**, 485 (1998).
[10] B. Ratra *et al.*, Astrophys. J. **517** (1999).
[11] D. Eisenstein, W. Hu, and M. Tegmark, astro-ph/9807130 (1998).
[12] M. Tegmark, Astrophys. J. **514** (1999).
[13] *http://map.gsfc.nasa.gov.*
[14] *http://astro.estec.esa.nl/sa-general/projects/cobras/cobras.html.*
[15] R. E. Lopez, S. Dodelson, A. Heckler, and M. S. Turner, Phys. Rev. Lett. **82**, 3952 (1999).
[16] M. Kaplinghat, R. J. Scherrer, and M. S. Turner, Phys. Rev. D **60**, 023516 (1999).
[17] W. H. Kinney and A. Riotto, astro-ph/9903459 (1999).
[18] A. Liddle, A. Mazumdar, and J. Barrow, Phys. Rev. D **58**, 027302 (1998).
[19] M. Kawasaki and H.-S. Kang, Nuc. Phys. B **403**, 671 (1993).
[20] S. Dodelson, G. Gyuk, and M. S. Turner, Phys. Rev. Lett. **72**, 3754 (1994).
[21] S. Dodelson, G. Gyuk, and M. S. Turner, Phys. Rev. D **49**, 5068 (1994).
[22] J. Madsen, Phys. Rev. Lett. **69**, 571 (1992).
[23] M. Kawasaki *et al.*, Nuc. Phys. B **419**, 105 (1994).
[24] J. Bond and A. Szalay, Astrophys. J. **274**, 443 (1983).
[25] G. Steigman and M. S. Turner, Nuc. Phys. B **253**, 375 (1985).
[26] J. Bond and G. Efstathiou, Phys. Lett. B **265**, 245 (1991).
[27] M. White, G. Gelmini, and J. Silk, Phys. Rev. D **51**, 2669 (1995).
[28] S. Bharadwaj and S. K. Sethi, Astrophys. J. Suppl. **114**, 37 (1998).
[29] S. Hannestad, Phys. Lett. B **431**, 363 (1998).
[30] S. Hannestad, Phys. Rev. Lett. **80**, 4621 (1998).
[31] S. Hannestad, Phys. Rev. D **59**, 105020 (1999).
[32] M. Kaplinghat, R. E. Lopez, S. Dodelson, and R. J. Scherrer, astro-ph/9907388 (1999).
[33] R. E. Lopez, S. Dodelson, R. J. Scherrer, and M. S. Turner, Phys. Rev. Lett. **81**, 3075 (1998).
[34] G. G. Raffelt, hep-ph/9902271 (1999).
[35] G. G. Raffelt, *Stars as Laboratories for Fundamental Physics* (University of Chicago Press, 1996).
[36] R. N. Mohapatra and P. B. Pal, *Massive Neutrinos in Physics and Astrophysics* (World Scientific, Singapore, 1998), 2nd ed.
[37] F. Wilczek, Phys. Rev. Lett. **49**, 1549 (1982).
[38] D. B. Reiss, Phys. Lett. B **115**, 217 (1982).
[39] G. B. Gelmini, S. Nussinov, and T. Yanagida, Nuc. Phys. B **219**, 31 (1983).
[40] H. Albrecht *et al.*, Z. Phys. C **68**, 25 (1995).
[41] M. Kamionkowski, A. Kosowsky, and A. Stebbins, Phys. Rev. D **55**, 7368 (1997).
[42] M. Zaldarriaga and U. Seljak, Phys. Rev. D **55**, 1830 (1997).
[43] M. Zaldarriaga and U. Seljak, Phys. Rev. D **58**, 023003 (1998).
[44] D. H. Lyth and A. Riotto, Phys. Rept. **314**, 1 (1998).
[45] C.-P. Ma and E. Bertschinger, Astrophys. J. **455**, 7 (1995).
[46] E. Kolb and M. Turner, *The Early Universe* (Addison-Wesley, Reading, MA, 1990).
[47] U. Seljak and M. Zaldarriaga, Astrophys. J. **469**, 437 (1996).
[48] G. Jungman, M. Kamionkowski, and A. Kosowsky, Phys. Rev. D **54**, 1332 (1996).
[49] S. Dodelson, E. Gates, and A. Stebbins, Astrophys. J. **467**, 10 (1996).
[50] M. Zaldarriaga, D. Spergel, and U. Seljak, Astrophys. J. **488**, 1 (1997).
[51] J. R. Bond, G. Efstathiou, and M. Tegmark, Mon. Not. Roy. Ast. Soc. **291**, L33 (1997).
[52] M. Tegmark, A. N. Taylor, and A. F. Heavens, Astrophys. J. **480**, 22 (1997).
[53] W. Press, S. Teukolsky, W. Vetterling, and B. Flannery, *Numerical Recipes in C* (Cambridge University Press, Cambridge, 1990).
[54] J. R. Bond, A. H. Jaffe, and L. E. Knox, astro-ph/9808264 (1998).
[55] See Ref. [34] for a review of neutrino oscillation experimental results.
[56] The Boltzmann code used in this calculation was written by Robert Scherrer.
[57] Of course cosmic variance is not noise in the proper sense. It is an intrinsic part of the anisotropy, and is separated this way for convenience.